Microfluidic device for controlled ocular drug delivery

Carlos Lavado Carreira

Thesis to obtain the Master of Science Degree in

Biomedical Engineering

Supervisors: Prof. Vania Cristina Henriques Silvério
Prof. Esmeralda Sofia Costa Delgado

Examination Committee

Chairperson: Prof. João Miguel Raposo Sanches
Supervisor: Prof. Vania Cristina Henriques Silvério
Member of the Committee: Prof. Frederico Castelo Alves Ferreira

December 2022

Preface

The work presented in this thesis was performed at the Instituto de Engenharia de Sistemas e Computadores - Microsistemas e Nanotecnologias (Lisbon, Portugal), during the period March-October 2022, under the supervision of Prof. Vania Silverio. The thesis was co-supervised at Faculdade de Medicina Veterinária (Lisbon, Portugal) by Prof. Esmeralda Delgado.

Declaration

I declare that this document is an original work of my own authorship and that it fulfills all the requirements of the Code of Conduct and Good Practices of the Universidade de Lisboa.

Acknowledgments

I would like to thank my parents and brother for their friendship, encouragement and caring over all these years, for always being there for me and without whom this project would not be possible. To Cláudia, whom endured me in the bad, the good, and with whom I could count to unburden my stresses and let me vent through my worries. To Vania, more than being my supervisor, was my rock in this work, to whom I would come to with any doubt, fear and trouble and would always make it seem so easy afterwards and make me regain confidence to continue the work. To my dissertation co-supervisor Prof. Esmeralda Delgado for her insight, support and sharing of knowledge, for having proposed what would become this Thesis and for the availability in offering her time and resources in the Faculty of Veterinarian Medicine. To Mariana, Catarina and Petra for the joint lab work and helping me with the work I had in front, learning together the mysteries of hydrogel fabrication. To Rahill, for the various discussions and insights, always ready to go out of his way to try and help. I would also like to acknowledge my colleagues at INESC-MN, Débora, João, Pedro, Ismael, Carlo for help provided when needed and for discussions about work and possibilities.

To each and every one of you – Thank you.

Abstract

Proper drug concentration during treatment is a challenge faced in ocular diseases. The need for repeated administration of the drug over the course of days, weeks and even years, sometimes with 1- or 2-hours regularity, changes peoples' lives, and is more problematic when it is dependent on a third party, as is the case of domestic animals, elderly, children and disabled people. To mitigate this issue, in this work a microfluidic device composed of hydrogel and a monolayer of graphene with 320 μm is researched as an alternative, attempting to provide a controlled ocular delivery of drug, replacing the repeated administrations by its occasional substitution. The work focuses on the chronic dry eye disease in animals, for which there is not a viable cure and may require treatment for life. The device has a rectangular shape of 10 x 5 mm and is inserted in the cul-de-sac of the eye, with the graphene layer anterior facing and the hydrogel in contact with the conjunctiva and portion of cornea. The hydrogel composition includes hyaluronic acid, due to its lubricant and wound healing properties, as well as being a common element in the body, making it biocompatible and safe. The active component is present at 0.5 % w/v, 1 % w/v and 2 % w/v. Graphene growth conditions in Chemical vapour deposition (CVD) are studied and the resulting samples are characterized by Raman spectroscopy. *In-vivo* testing in the eye of a small dog was conducted as a proof of concept to test the device's biocompatibility and biofunctionality, with good results regarding the former and improvement needed in the latter, since the device was expelled in three different trials after a few hours. It is expected that such a device can positively impact the lives of animals suffering from the disease, alleviate worry of the animals' owners and be mass produced, eventually also crossing the barrier for human treatment as well.

Keywords

Resumo

A manutenção de uma concentração eficaz de fármaco é um desafios no tratamento de doenças oculares. A necessidade de administração repetida ao longo de vários dias, semanas e mesmo anos, com uma posologia por vezes tão regular como a cada hora, altera as vidas das pessoas. É mais problemático quando há dependência de terceiros, como no caso dos animais domésticos. Neste trabalho, um dispositivo microfluídico, de composição de hidrogel e uma monocamada de grafeno, com 320 μm é desenvolvido como alternativa, com o intuito de substituir as repetidas administrações de gotas pela ocasional substituição do dispositivo por um novo. O trabalho incide no olho seco em animais, uma doença crónica para a qual não existe ainda uma cura viável e pode requerer tratamento para a vida. O dispositivo apresenta forma rectangular 10 x 5 mm e é inserido no saco conjuntival do olho, com a monocamada de grafeno virada para o saco conjuntival e o hidrogel em contacto com a conjuntiva e parte da córnea. É adicionado ácido hialurónico ao hidrogel como composto activo, com uma concentração de 0.5 % w/v, após testes com 0.5 % w/v, 1 % w/v e 2 % w/v, devido às suas propriedades lubricantes e cicatrizantes, para além de ser biocompatível, já existindo naturalmente no corpo. As condições para o crescimento de grafeno são estudadas e este é caracterizado com espetroscopia de Raman. Foram realizados testes *in-vivo* num cão de pequeno porte de forma a testar a biocompatibilidade e biofuncionalidade do dispositivo, com obtenção de bons resultados na biocompatibiliade, mas mostrando necessidade de refinamento das dimensões para melhorar a biofuncionalidade. O dispositivo saiu do olho nas três tentativas efectuadas ao fim de umas horas. É esperado que um dispositivo deste tipo consiga impactar de forma positiva as vidas dos animais que sofrem da doença, podendo também vir a ser utiliizado em medicina humana.

Palavras Chave

Dispositivos microfluídicos; administração tópica ocular de fármacos; hidrogel; grafeno; ácido hialurónico.

Contents

List of Figures

List of Tables

Listings

Acronyms

3D	Three dimensional
ALS	Asymmetric least square
Patm	Atmosferic pressure
c-Si	Crystalline silicon
CTAB	Cetyltrimethylammonium Bromide
CVD	Chemical vapour deposition
DI	Deionized
DED	Dry Eye Disease
EGDMA	Ethylene glycol dimethylacrylate
HA	Hyaluronic acid
HEMA	Hydroxyethylmethacrylate
ICS	Intensity Correction System
INESC MN	Instituto de Engenharia de Sistemas e Computadores - Microsistemas e Nanotecnologias
IOP	Intraocular pressure
IPA	Isopropyl alcohol
MAA	Methacrylic acid
PDMS	Polydimethylsiloxane
pHEMA	Poly (2-hydroxyethyl methacrylate)
PI	Photoinitiator
PLA	Polylactic acid
PMMA	Poly(methyl methacrylate)
RPM	Rotation per minute

sccm	Standard cubic centimeters per minute
SEM	Scanning electron microscopy
STF	Simulated Tear Fluid
STT	Schirmer tear test
SVG	Silicon Valley Group
UV	Ultraviolet

1

Introduction

Contents

The introduction chapter gives a little context of the research area, from the approached disease and available treatments, to the properties of Hyaluronic acid (HA) and the advantages in using it. It also mentions the main points of graphene synthesis, characterization and extraction.

1.1 Motivation

When faced with a disease needing treatment, proper drug administration is key for a fast and good recovery, or even to properly manage the symptoms in case of chronic diseases. In ocular treatment, due to the particularities of the eye, drug administration faces some challenges with keeping proper concentration and thus, ensure a good treatment. Trying to reduce the number of administrations, the concentration tends to be higher and shoot over the maximum safety concentration, then stay for a while in the desired range and finally fall bellow the minimum effective concentration. Using less concentration and more frequent administration improves the time when the drug is between these concentration limits, but requires availability of the person, and when dealing with third party dependency, as in the case of domestic animals, elderly, children and disabled people, that are not autonomous, many times the treatment is not properly given. By researching and developing new treatments and new devices that take away a significant burden in the caretaker, it helps to increase quality of life, not only for the patient, but also for those around him. To adress this issue, we aimed to develop an ocular drug delivery device based on microfluidic technology to allow for drug sustained release in chronic conditions, without the need of frequent administration of eye drops.

1.2 State of the Art

1.2.1 Chronic dry eye disease treatment

Dry Eye Disease (DED) is a condition affecting the proper lubrication of the eyes. It can be caused by a decrease in tear creation or increase in tear evaporation, that can lead to damage to the corneal surface and declining vision. The decrease in tear production can be caused by autoimmune or inflammatory systemic conditions, that damage the tear glands and the increase in evaporation can be caused by production of low-quality tears, that have less constituents to hold the water in the eye and prevent it from evaporating.

Usual treatment for DEDs include artificial tears, warm compresses and changing some habits, reducing stresses in the eye, for example using less aggressive shampoos [1]. Many of the common artificial tears include HA in its constituents since it is already distributed widely throughout connective, epithelial, and neural tissues and serves the purpose of lubrication and also wound healing [2]. A

common compound with regular clinical use is topical cyclosporine A, an anti-inflammatory drug, that is used when the more usual treatments fail, but is however very expensive and has a significant rate of secondary effects [3]. More recently, due to the similarities between serum and natural tears, that include antimicrobials, growth factors, lipids and proteins, platelet derived products, employed in tissue regeneration and wound healing, have been used in DED, showing improvements in symptoms and clinical signs [4, 5]. For patients that have a significant component of meibomian gland dysfunction and evaporative dry eye disease, procedures using heat or mechanical energy have been used to restore natural flow of meibum and express glands [6, 7]. Several devices exist as an option to treat DED. The intranasal tear neurostimulation TrueTear®, that was designed to stimulate, via small electrical currents, the mucosal nerves through the nasolacrimal reflex pathway [8]. Scleral lenses, that rest on the sclera, creating a reservoir over the cornea and protect it, as it is more sensitive [9]. Another device uses amniotic membranes, that provide coverage of the epithelium, allowing it to heal, and also have anti-inflammatory properties [10]. Contact lenses soaked in drug solutions or more engineered to have incorporation of the drug during its fabrication are also being explored for prolonged use, serving as a means of alternative delivery [11–13].

1.2.2 Hyaluronic acid laden hydrogel for ocular applications

Fabricating hydrogel lens or lens like materials are an enormous world of possibilities, that spawns from the range of available polymers, to the formula of components in a recipe, to different polymerization techniques that form the same polymer (radical or catalytic polymerization, among others) and the polymerization conditions (temperature, initiator, vessel, etc.) can be set to impose different properties on the polymer. Hydroxyethylmethacrylate (HEMA) hydrogels for one, are inexpensive, biocompatible and have a high number of copolymer possibilities, but have a low oxygen permeability and face protein adsorption issues. The copolymer possibilities may in fact solve the negative aspects, by contributing with their own set of advantages [14].

Due to the ubiquitous presence in the body and water retention properties, HA has many ophthalmology related applications, among them the treatment of DED and contact lens incorporation as an additive, from being included in the production material to surface coating and as a multipurpose solution. It can be used in *in situ* gels, nanoparticles, as intravitreal injection or in tissue engineering. More specifically, in its applications on contact lenses, by modifying the surface roughness of the lens, and enhancing surface water retention, while reducing protein adsorption onto the lens, and improving biocompatibility [15]. Since contact lens are widely used, are convenient and inexpensive to make, using them as delivery vehicles is a natural step. Entrapping HA in contact lenses to prolong the duration of release, have shown results of up to 15 days of release [16]. HA can also assist in drug release, by promoting a more complete release of another drug that is incorporated in conjunction with it in the lens,

and they don't alter significantly the hydrogels characteristics [17].

1.2.3 Quantification of Hyaluronic Acid

The main method used for quantifying HA in biological fluids has been the carbazole assay. In culture broth it is however difficult to measure the concentration of HA due to reactions that arise from glucose and polysaccharides present. There is the necessity of removing them first, to get correct readings. It is the most used method for uronic acid measuring for example, through reaction of the uronic acid with the carbazole. This method is based on the principle that when treated with acid solutions like HCL or H_2SO_4, carbohydrates yield mixtures of products that react with the carbazole and give different colors. To extract and purify HA to measure its concentration with the carbazole assay, it is a very laborious and time consuming endeavour.

There is another method however, the turbidity assay, that relies on the principle of precipitation of polyanions by organic ammonium cations. By usage of Cetyltrimethylammonium Bromide (CTAB), that form insoluble complexes with the HA producing turbidity, the amount of which is proportional to the concentration of HA in the solution. It doesn't require the purification steps the carbazole assay does, making it much simpler and less laborious, without loss in viability of results [18].

1.2.4 Graphene growth by Chemical Vapour Deposition

The most established and usual method to grow high quality graphene films in a large area, that also happens to be the most convenient methodology, is Chemical vapour deposition (CVD) [19]. The process has a major drawback, as it needs a metal catalytic substrate, usually Cu or Ni, upon which the graphene grows, making it necessary to extract and transfer the graphene onto the final substrate afterwards. There are protocols that enable this transfer process [20–22], but the manipulation induces structural and chemical defects that limit its intended applications. The mechanism used for growth of graphene involves usually a deposition gas (hydrocarbon) such as methane or acetylene, and a metal catalyst substrate. At temperatures near the melting point of the substrate a reaction for the nucleation of graphene is catalysed, When the solubility of carbon is very low on the substrate, as in the case of Cu, a surface-adsorption growth of graphene dominates the process. This growth is self-limited, meaning that the graphene growth is terminated when the Cu surface is fully covered, losing the catalytic role it had in decomposing the deposition gas, that provides the carbon source [23]. A reducing gas, usually H_2 is used, having a role in counterbalancing oxidation of the substrate by cleaning the oxygen containing impurities due to its reducing effect, while also controling the substrate's grain size and dimension by etching weaker carbon-carbon bond, but too much partial pressure of hydrogen has the contrary effect, degrading the quality of graphene growth [24, 25]. An inert gas, such as Ar, is used as a supporting

agent, diluting the deposition and reducing gases and directing them to the substrate. The process can be done at low pressure (LPCVD), atmospheric pressure (APCVD), and plasma enhanced (PECVD), depending on the machine capabilities and conditions intended. The machine itself can be hot wall or cold wall, meaning that the entire chamber is heated or, in the latter, only localized heating of the substrate is done. By using low pressures, the volatility of the substrate increases, reducing the temperature at which the substrate sublimates, and the activation energy for graphene nucleation decreases [26,27]. The nucleation density is fundamental, since it determines domain sizes, that have crucial roles in the graphene quality. Decreasing this density means that larger graphene domain sizes are achieved and a better graphene surface continuity with less defects results from it. By focusing on substrate treatment and conditioning, less impurities and defects are present, and better grain size and crystalline arrangement can be obtained, which in turn helps in the decrease of nucleation density [27]. The substrate treatments and conditioning can vary from pre-treatments of the substrate to add oxidation layers and electropolishing to remove defects [28], to annealing temperature and duration, partial gases flow during graphene growth, and growth duration [29].

1.2.5   Graphene Characterization by Raman Spectroscopy

Among all the characterisation techniques used for graphene, Raman spectroscopy plays a major role mainly due to its simplicity and range of information that can be obtained. A powerful technique that is fast, non-destructive and with high resolution, it can be used to determine the orientation of the layers and their number, the quality of the edges and its types, and even effects of different perturbations, such as electric and magnetic fields. Raman scattering on phonons is determined by the electrons movement interference and scattering, meaning that variations of electronic properties due to defects, doping, edges and magnetic fields will affect the position, width and intensities of Raman peaks. Graphene is therefore an excellent material for the technique as all wavelengths of incident light are absorbed resonantly. Since there is no energy band gap, the interaction between the electronic sp^2 system and the phonon spectrum outputs make it easy to identify the fingerprint in a Raman spectrum [30]. Two strong peaks are usually present in the Raman spectrum of quality graphene, the G and 2D modes, with a third peak appearing if the laser beam focuses on edges or defects of the graphene, the D mode. G mode is an interaction through electron-hole single resonance, while the D and 2D modes are intervalley double resonance [31]. The G peak intensity is proportionally dependent with the number of graphene layers, the D peak with the grain boundaries and defects present and the 2D peak appears if there is graphene present, being a characteristic of its quality. Having one defined 2D peak signals the presence of monolayer graphene, while the increasing number of layers will influence the peaks' position and intensity, increasingly shifting to the right with the increase in layer numbers. The peaks positioning, that are the most intense features in the graphene's Raman spectrum are at 1345 cm^{-1} (D peak), 1585

cm^{-1} (G peak), and 2690 cm^{-1} (2D peak) [32, 33]. The peaks intensity ratio is also a measure of the quality of the graphene and number of layers, where a low I(D/G) (¡0.5) and high I(2D/G) (2-4) ratios are indication of high quality [34].

1.2.6 Graphene Extraction

Three main processes are used for graphene extraction from metal substrates. Electrochemical bubbling, oxidative decoupling transfer and the most used technique, chemical wet etching. In all of these methods there is a step where a protective polymer layer is spin-coated on top of the graphene surface, that provides mechanical support, so that the graphene film remains intact after the substrate is extracted. The stronger interaction between the polymer and graphene also contributes towards facilitating the extraction of the graphene from the substrate.

Chemically wet etching the substrate is usually a fast and straightforward method to use, given the right etching solution for the metal that is being used as substrate. It implies the loss of the substrate and of one of the sides of graphene, which is a major concern in up-scaling graphene production. After the protective polymer layer is added to one of the sides of the substrate/graphene stack (graphene usually grows on both sides), the other side is etched by O$_2$ plasma, by interaction of the plasma with the carbons of the graphene, removing it. After plasma etching the exposed side, the stack substrate/-graphene/polymer is introduced in an etching solution to remove the substrate. After this step, the remaining impurities and residues left are cleaned in a series of solvents and Deionized (DI) water, leaving the graphene/polymer stack ready to be transferred onto the final substrate [35, 36].

To use the electrochemical bubbling method, it is necessary to setup the substrate as the cathode in an electrochemical cell, complementing it with an anode, place them in a chemical solution and apply tension to the cells. The electrical tension promotes oxidation in the substrate, producing bubbles that will promote the release of the graphene layers from the sides of the substrate. It is a non destructive method, that allows for the reuse of the substrate and manages to keep both graphene layers intact, potentially doubling the yield. It is also a cleaner method, leaving fewer impurities in the graphene surface. The method does however involve many parameters that need fine tuning to be able to remove the graphene without damaging it [37, 38].

The oxidative decoupling transfer is used to extract graphene in the specific case of thin copper films, that are usually sputtered in another substrate, for example oxidized silicon. It is a method similar to the previous, but without the bubbling, preventing the thin film from delaminating from the adhered substrate. It is also a non destructive method, allowing to reuse the substrate, which is of higher crystallinity and purity, per norm [39].

1.3   Organization of the Document and specific objectives

This thesis is organized as follows: Chapter 1 includes a brief context of the state-of-the art of the dry eye disease treatment, the usage of hydrogel lens and lens like materials, the extent recourse to HA and its quantification. Chapter 2 is separated in four sub-sections: protocol for hydrogel fabrication, graphene growth, characterization and extraction, assembly and characterization of the insert and the *in-vivo* testing of the insert, approaching general procedures and protocols, techniques, machine operations and detailing the composition of solutions and their fabrication. Chapter 3 presents all the trials that were done, their results and a brief discussion about them and the decisions taken. It goes through the development of the work, the issues and solutions. Chapter 4 presents the main conclusions of this thesis including proposed future work to be developed.

2

Materials and Methodology

Contents

The present chapter includes a description of the different techniques used for the fabrication of the device, from hydrogel fabrication to graphene growth and characterization, preparation of solutions and different protocols used during and before trials.

2.1 Materials

List of reagents used:

	Formula	State	CAS	Purity (%)	Manufacturer
Sodium acetate	C2H3NaO2	Solid	127-09-3		Sigma-Aldrich
Sodium hydroxide	HNaO	Solid	1310-73-2	0,98	Acros Organics
Hyaloronic acid	C14H21NO11	Solid			Shandong Topscience Biotech Co., Ltd
2-Hydroxyethyl methacrylate	C6H10O3	Liquid	868-77-9	-	Sigma-Aldrich
Methacrylic acid	C4H6O2	Liquid	79-41-4		Sigma-Aldrich
Ethylene glycol dimethacrylate	C10H14O4	Liquid	97-90-5		Sigma-Aldrich
Diphenyl(2,4,6-trimethyl--benzoyl)phosphine oxide	C22H21O2P	Liquid	75980-60-8	0,98	Tokyo Chemical Industry
Acetic acid	C2H4O2	Liquid	64-19-7	99.9	VWR Chemicals
Cetyltrimethylammonium bromide	C19H42BrN	Solid	57-09-0		VWR Chemicals
Sodium chloride	NaCl	Solid	7647-14-5		Sigma-Aldrich
Sodium hydroxide	NaOH	Solid	1310-73-2	0,98	VWR Chemicals BDH

2.2 Methodology

2.2.1 Protocol for hydrogel fabrication

The Poly (2-hydroxyethyl methacrylate) (pHEMA) based hydrogel was synthesised by free radical polymerization with precursors HEMA as the main monomer and Methacrylic acid (MAA) as the second monomer. The crosslinking agent used was Ethylene glycol dimethylacrylate (EGDMA), the photoinitiator was Darocur® (2, 4, 6-trimethyl benzoyl-biphenyl-phosphinoxide) and DI water was added to the mix. The active compound HA was added to the hydrogel formulation to be released by diffusion for the treatment of dry eye disease.

The protocol was done as follows:

Two solutions are prepared. In the first, the HA in powder was mixed by hand with water at ~ 4 °C, vigorous mixing was done at 2h intervals for 6 h and then kept to rest at least 10-12 h to allow fully dissolution and homogenization, always keeping it at ~ 4 °C in the fridge. The other reagents were mixed in a second solution in the following order: HEMA, MAA, EGDMA and the Photoinitiator (PI) using a magnetic mixer until the PI powder is fully dissolved.

Then both solutions are mixed and sonicated in an ultra-sonic bath to remove air bubbles. If HA is poorly dissolved in the mix and sonication, then the solution is stored in the fridge to allow HA to dissolve again. The hydrogel mix is then ready to be spread onto the substrate for a given thickness and exposed under Ultraviolet (UV) light for polymerization.

Three methods were tested to spread the hydrogel into a uniform layer of 60 to 80 μm and of 320 μm. The first approach consisted in spin-coating the hydrogel (section 2.2.1.A). The centrifugal forces acting on the liquid, drive the liquid outwards. The rotation speed and time will define the film thickness. A given volume of solution is poured on top of a flat substrate and rotated for a given time and velocity. In the second approach a set volume of hydrogel was pipetted onto a flat substrate and let to flow and spread on the surface by the action of cohesive and adhesive forces (section 2.2.1.B). The third method used, a Poly(methyl methacrylate) (PMMA) mold was fabricated, into which the solution is cast and sealed with a PMMA cover, to define shape and thickness, and cured (section 2.2.1.C). Different materials were studied as substrates: glass, PMMA and acetate sheet. Surface treatment with O_2 plasma was also performed and its effect studied. The glass substrate used was Hirschmann Deckglases 24x50 mm and 0.13-0.17 mm thick.

The methodology to extract the polymerized hydrogel from the substrate was also addressed. Trials were done with the hydrogel in hydrated or dehydrated form and using different solvents (acetone, ethanol and Isopropyl alcohol (IPA)), depending on substrate compatibility.

In the various steps described it is always important to have clean substrates and surfaces. For that reason, the usual cleaning protocol is as follows, except if there is an unwanted reaction between solvents and substrates:

- Clean surface with acetone;

- Clean surface with IPA to remove acetone residues;

- Clean surface with DI water;

- Dry with aid of the compressed air pistol.

2.2.1.A Spin-coating

Spin-coating is extensively used in microfluidics and microfabrication for spreading a liquid or solution onto a substrate for a given thickness. Examples found in microfluidics often use Polydimethylsiloxane (PDMS) or SU-8 photoresist [40]. The same rational was used here, starting with known conditions for SU-8 and for PDMS used at Instituto de Engenharia de Sistemas e Computadores - Microsistemas e Nanotecnologias (INESC MN) fabrication protocols and optimizing them to the hydrogel solution.

The testing and optimization was done for the mixture of pHEMA without HA, as used throughout the work since the solution presents very low viscosity for spin-coating. As such, an intermediate step of

pre-curing by UV was added. A UV-KUB 2 (365 nm $\pm$ 5 nm wavelenght), a compact exposure-masking system equipped with a UV LED based optical head that is collimated and homogeneous, was used for UV exposure (pre-curing step). This same machine is further used for the polymerization of the hydrogel.

The first trials were done using a Laurell spin-coater model WS-650MZ-23NPP/LITE, that has already some settings in memory for the most common uses of the machine, namely with PDMS and SU-8. Two programs were used, that were optimized for SU-8 spreading, P4 and P5. Then, new conditions were introduced, PH1, PH2, PH3 and PH4, to test for different conditions both in the spreading and in the thickness definition steps. The detailing of the programs used can be seen in Table 2.1.

In the trials that used the Laurell spin-coater, the substrate was secured with Kapton tape onto a wafer and the wafer is mounted on the spin-coater's vacuum nozzle.

Table 2.1: Different programs used for spin-coating. In the initial spreading, the liquid is evenly spread across the surface of the substrate, and then a higher velocity is imposed to define the flow thickness. Programs S1 and S2 are converted into G-code, used to define the parameters in the Arduino board.

Program	Initial spreading		Thickness definition	
	Time (s)	RPM	Time (s)	RPM
P4	5	500	20	2200
P5	5	500	20	1200
PH1	5	500	20	1700
PH2	5	500	20	800
PH3	5	100	20	800
PH4	5	100	20	300
S1	5	100	20	300
S2	5	500	10	300

A different setup was mounted afterwards, consisting in a stepper motor controlled by an Arduino, Figure 2.1, using a driver and G-code commands to set the spin-coating speeds (range) to obtain the required flow thicknesses. The commands used were as follows:

- G0 - tells the motor to move.

- X - tells the motor how much to move. A full revolution is X1.6, with each full revolution being a multiple of 1.6.

- F - sets the feed rate of the motor, that translates into Rotation per minute (RPM). In this setup F136.8 is equivalent to 100 RPM.

It was necessary to know the correspondence between input feed rate to output RPM, so a set of tests was conducted by inputting increasing feed rates, recording videos and processing the information to obtain a calibration curve. The videos were recorded with a Levenhuk Digital Microscope (frame rate = 30 fps, format = 1280x720, 2 megapixels) using MicroCapture software and processed in Matlab® R2019a, using a script developed on the basis of a preexisting code (Appendix C).
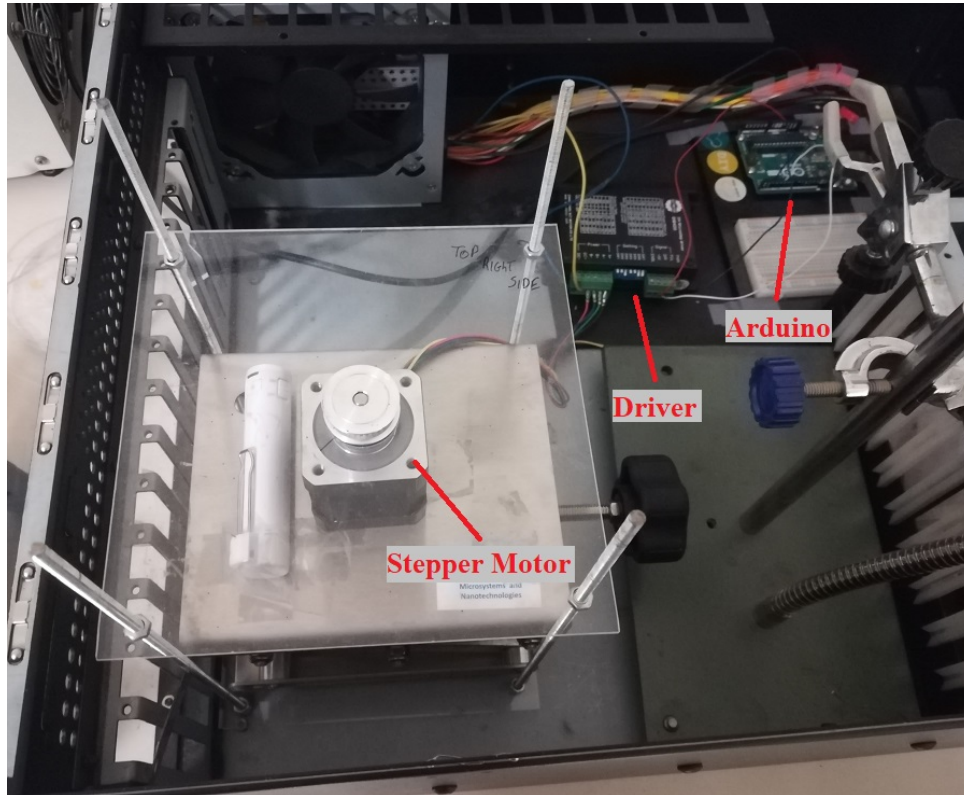
Figure 2.1: spin-coating - Setup showing the stepper motor controlled by Arduino through the driver

2.2.1.B   Wetting and spreading

Trials for the deposition of solution onto a substrate using a micropipette for a given thickness defined by wetting and spreading were done for different volumes of solution deposited. The prepolymer solution is pre-cured to increase viscosity. Three different substrates were used: PMMA, glass and acetate sheet. PMMA and glass surface were further treated by O2 plasma. The process consists in cutting the surfaces, clean them with IPA and water and submit them to a plasma.

2.2.1.C   Casting

The hydrogel was also cast onto a mold designed and fabricated in PMMA (100x100x5 mm) using a milling machine. The design was made using FreeCAD 0.20 and finalized in AutoCAD. The design translated into G-Code and run in the milling machine with the help of MACH2 sofware. The fabrication protocol can be found in appendix B. The mold was then engraved using a FLUX Beambox laser cutter (Speed = 150 mm/s, Power = 25 %). The bottom and top lids were designed in Beam Studio v1.8.3 and cut also in the laser cutter (Speed = 8 mm/s, Power = 60 %). Both the design and end result can be seen in Figure 2.2.

The bottom lid, with a thickness of 2 mm, was placed inside the mold, which is 2.8 mm deep. Then
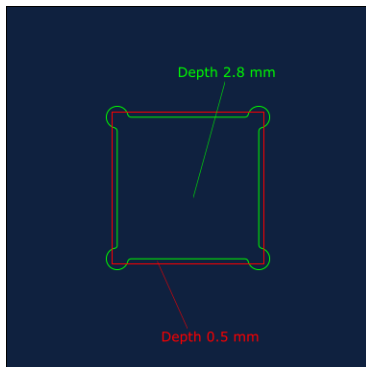
(a) CAD design front view of Mold_V1, made in FreeCAD
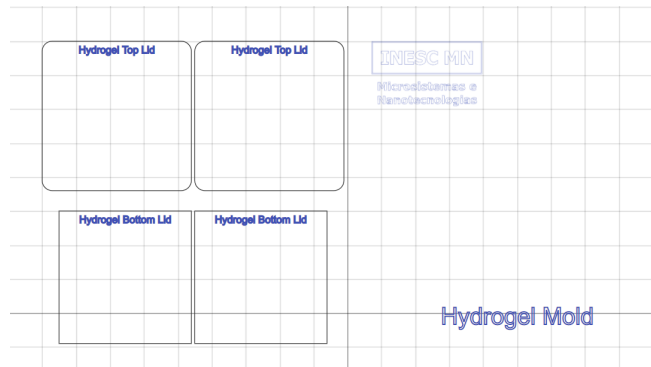
(b) Engraving design and bottom and top lids, made in Beam Studio
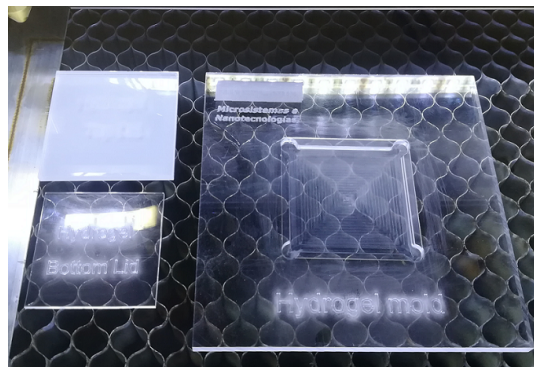
(c) Mold_V1 finished with bottom and top lids, engraved and final cuts done in the Flux Beambox laser cutter

Figure 2.2: First version of the PMMA mold

the top lid is placed on the top edge, which is 0.5 mm deep, and the gap between the two lids is $2800 - 2000 - 500 = 300 \ \mu m$.

Improved versions of the PMMA mold designs, seen in Figures 2.3(a), 2.3(c) and 2.3(e), were done in the Beam Studio v1.8.3, cut and engraved using the laser cutter (Cut: Speed = 8 mm/s, Power = 60 % || Engrave: Speed = 150 mm/s, Power = 25 %). A spacer (CROMOlab chromatography fibers with 320 μm diameter) is used to define the thickness of the hydrogel. Here the bottom lid is bigger than the hole of the main piece and is tapped onto the backside of the mold. The spacers are placed in the corners of the mold and the top lid is placed on top of the spacers and inside the mold.

2.2.1.D Polymerization of the prepolymer solution using Ultra Violet light

After having the precursor solution of hydrogel on the substrate, the hydrogel was polymerized using UV light (Figure 2.4). The machine has controllable exposure time, radiation power and can do continuous or
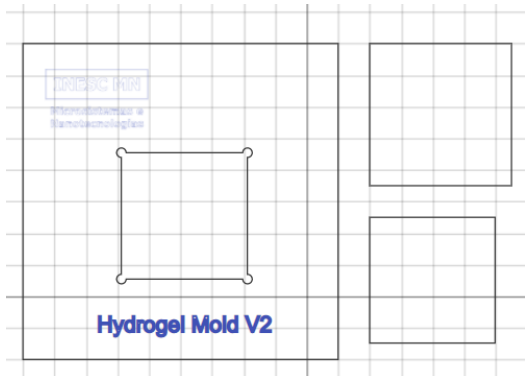
(a) Design of Mold_V2, top and bottom lids
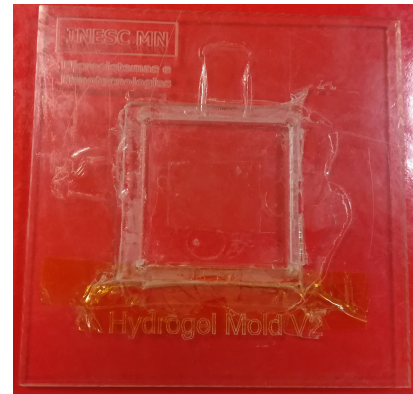
(b) Mold_V2 with bottom lid taped in the underside
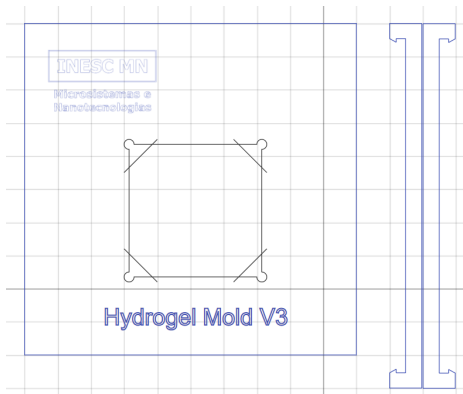
(c) Design of Mold_V3 and securing arms
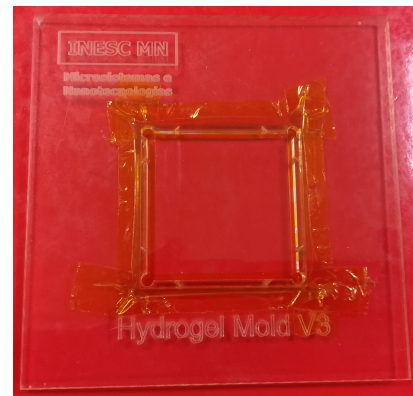
(d) Mold_V3 with bottom lid taped in the underside
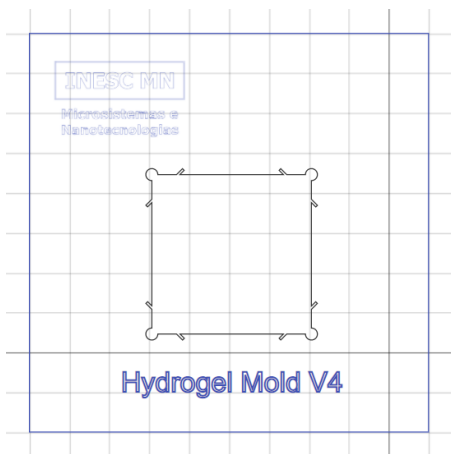
(e) Design of Mold_V4
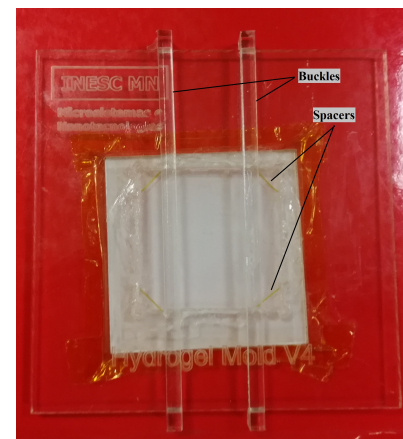
(f) Mold_V4 with bottom lid taped in the underside, spacers in the corners and buckles on top

Figure 2.3: Iterations on the PMMA mold design

cyclic exposure with ON and OFF periods. Tests with conditions presented in table 3.1 were performed until an optimal set of conditions were achieved for the hydrogel to polymerize. The UV exposure system and optimal conditions were used in all subsequent polymerizations.

When a sufficient exposure time for the set power is achieved, the hydrogel is polymerized. This UV exposure system was also used in all polymerization pre-curing steps of the different trials.
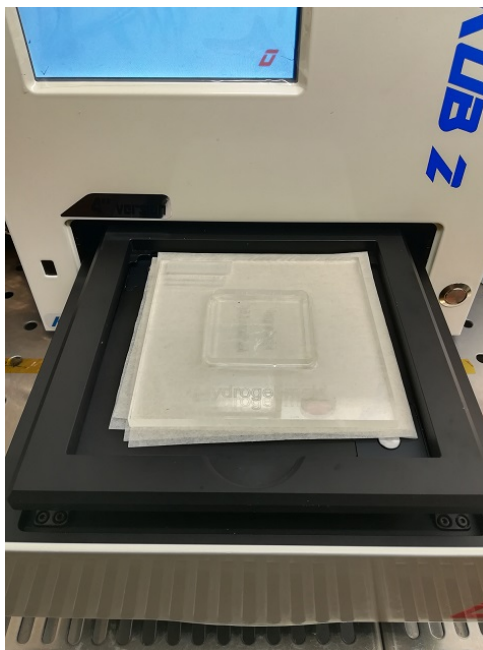
Figure 2.4: Prepolymer solution casted in the PMMA mold V1. The assembly is loaded into the UV-Kub 2 drawer, for photo polymerization

Typical pre-curing conditions defined for this process were 1 min 5 s at 30% power in a full surface continuous exposure (ON). The first set of conditions for polymerization was chosen based on the work of [13] and [41]. Based on these studies, several tests (table 3.1) were performed, after which was settled on a cyclic exposure consisting of 200 cycles with 2 s ON and 1 s OFF and later with the use of the molds, it was settled on 8 cycles with 2 min ON and 30 s OFF, totalling 20 min (16 min of effective exposure with a radiation power of 10.5 mW/cm$^2 \pm 10\%$). This was done to prevent heating of the LED that would consequently heat the environment and the sample.

2.2.2 Graphene Growth, extraction and characterization

2.2.2.A Graphene Growth

The graphene layer that will bond with the hydrogel layer was grown in an Aixtron Black Magic 2" CVD (fig. 2.5). This machine is a dedicated furnace for graphene synthesis which has a cold wall heating system, meaning that only the holder where the substrate is placed is heated, and not the entire chamber.
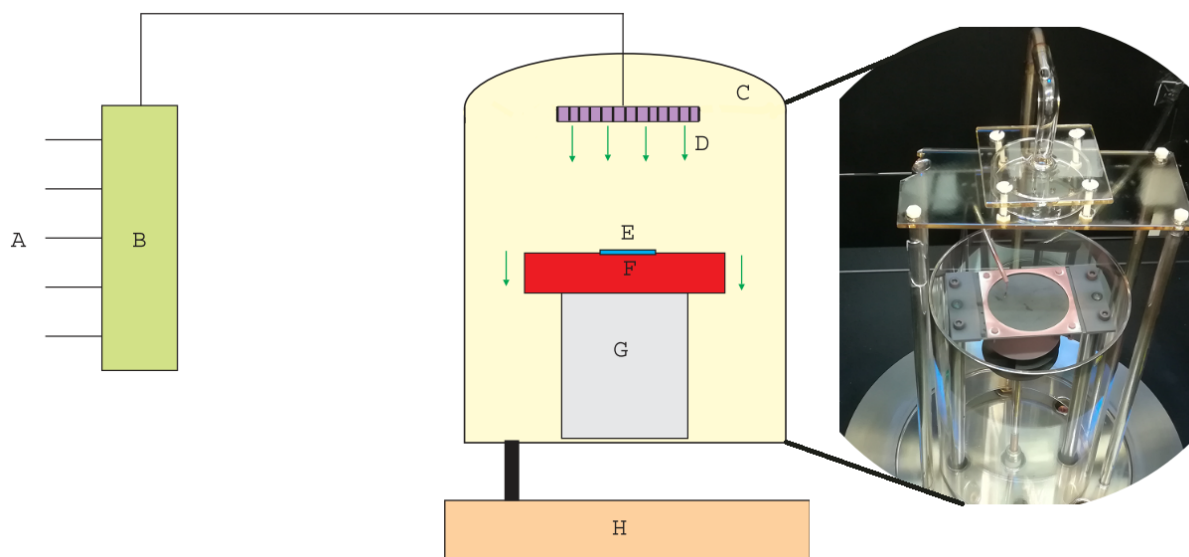
Figure 2.5: Schematic design [42] of the Aixtron Black Magic 2" CVD and image of the reaction chamber. The process gases enter (A) and are mixed in the gas mixing system (B) before being fed into the chamber (C) via the showerhead (D). The substrate (E) is heated by the graphite heater (F) and the chamber's pressure is regulated through the pressure control system (H). A deposition shield to provides a sacrificial surface (I) [42].

The heater is made of graphite and is required to heat the metal catalyzer (the substrate) to a sufficiently high enough temperature for the surface reaction to occur and graphene to start growing.

The graphite heater can reach a maximum temperature of 1000 °C, induced by Joule effect and controlled by a closed loop proportional–integral–derivative controller using a thermocouple in contact with the heater surface. It has the capacity to set a range of heating and cooling ramps between 1 - 999 °C/min controlling the current, voltage and power output that reaches the graphite.

The chamber has a pressure control system, for pressure range between 1 - 720 mbar, with a varied array of valves that control chamber venting and pumping of gases. The gases used in this work for the processes are methane (CH_4) as the precursor for the growth reaction, hydrogen (H_2) that improves the cleavage of the H-C bond in CH_4 and sputters the substrate surface to remove impurities and oxidation, argon (Ar) as an inert carrier, and nitrogen (N_2) as the ballast gas to dilute process gases. For each gas there is a mass flow controller within the range of 0 to 9999 Standard cubic centimeters per minute (sccm), but are factory calibrated for 1000 sccm H_2, 500 sccm CH_4, and 1000 sccm N_2 [42].

The machine has an interactive interface and its software monitors in real time the different parameters being set and read from the sensors. In addition it has a camera which allows the visualization of the process in the chamber.

The substrate, that acts as the catalytic material for the reaction promoting the graphene growth, is Cu foil with 99.999% purity (25 mm width x 0.025 mm thickness Alfa Aesar). During the annealing step the size of the grains of Cu increase and its lattice rearranges into a more stable configuration

18

(1,0,0), improving the yield of graphene growth [27]. The temperature for graphene growth should be set at 1000 °C, close to the melting temperature of Cu, at Atmosferic pressure (Patm). The process is imposed to occur at pressure lower than Patm (20 mbar) at which the volatility of Cu increases allowing it to sublimate at lower temperatures [26]

For the machine and parameters control, programmable recipes in the machine's language can be created by the user and are divided into the following main steps:

- Initial cleaning of the substrate surface with an Ar flow (fig. 2.6 - A)

- Setting of the temperature ramp to heat the substrate up to the process temperature (fig. 2.6 - B)

- Annealing of the substrate after reaching and maintaining the process temperature. Both Ar and H_2 gases flow one imposed to the chamber (fig. 2.6 - C)

- Growth of graphene with the introduction of the precursor gas, CH_4, at the same temperature as the annealing (fig. 2.6 - D)

- Cooling ramp to room temperature (fig. 2.6 - E)
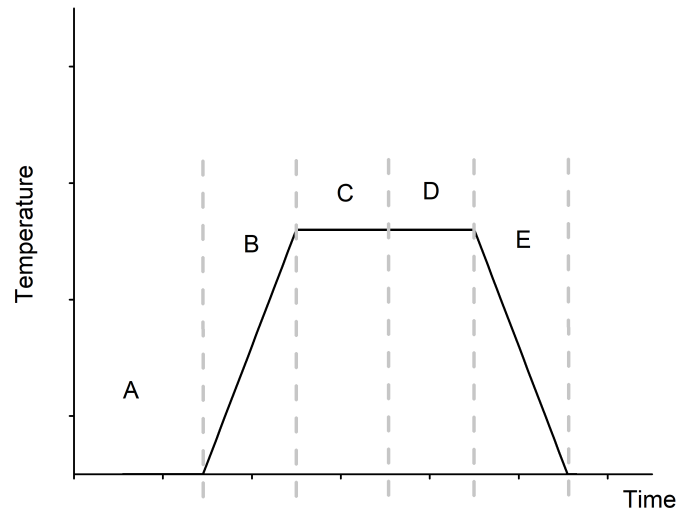
Figure 2.6: Schematic detailing the main steps to CVD graphene growth as a function of time and temperature.

The conditions of main recipes tested for graphene growth are in Appendix A. An example of set parameters has the process temperature and pressure for annealing and growth (T = 825 °C and P = 20 mbar), annealing time = 10 min, graphene growth time = 10 min, H_2 flow = 20 sccm, Ar flow = 560 sccm and CH_4 flow = 10 sccm.

19

2.2.2.B Graphene Extraction

The graphene grown in the previous section is transferred to the hydrogel. This transfer was optimized using three different protocols, schematized in fig. 2.7. One of the protocols tested starts by spin-coating a PMMA 950 layer on top of the graphene using a Silicon Valley Group (SVG) 88 Resist Coat Track. The PMMA is baked. These two steps are repeated to obtain a thicker layer of PMMA of 1.2 μm. The PMMA layer will serve as a support for the graphene film after the Cu is removed by chemical wet etch.

Now with the stack Cu/graphene/PMMA, the Cu substrate is chemically etched in a solution of 0.5 M Iron(III) chloride hexahydrate (FeCl$_3$.6H$_2$O) until complete Cu etching.

Cleaning steps follow, the graphene/PMMA stack is cleaned in consecutive steps starting by fishing it from the FeCl$_3$.6H$_2$O solution with the aid of a glass slide and placing it in a beaker with DI water. Then the stack is transferred onto a 2% Chloridric acid (HCl) solution for 30 min. This transferring of the sample between DI water and 2% HCl is performed three times. The stack is then placed in DI water to clean the acid residues before being transferred onto the hydrogel.
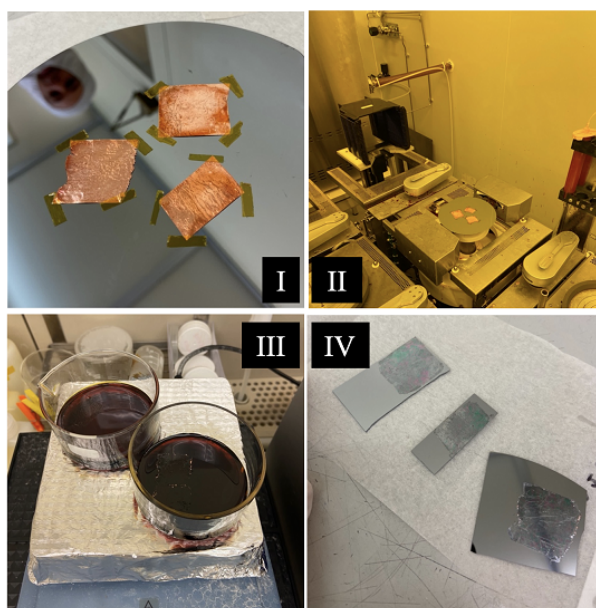
Figure 2.7: The samples of Cu/graphene stack are secured to a Si wafer with use of Kapton tape, **(I)**, then the samples are coated in the SVG track with PMMA, **(II)** and after curing the PMMA the samples are added to a solution of $FeCl_3 \cdot 6H_2O$ for the etching of the Cu layer, **(III)**. After etching the graphene/PMMA stacks go through the cleaning steps and are transfered onto the final substrate, **((IV)**

In the second protocol, the stack PMMA/graphene is fished directly to the hydrogel, and the cleaning step is performed as before. In the third protocol, the PMMA support layer is replaced by the prepolymer solution of hydrogel for a stack Cu/graphene/hydrogel. The hydrogel is polymerized in UV on UV-KUB 2. The chemical etch of Cu and the stack cleaning was done as previously. An overview of the different protocols can be seen in Figure 2.8.

The protocol optimized after these testes can be found in Appendix D, and an overview of the main steps is seen in fig. 2.7.
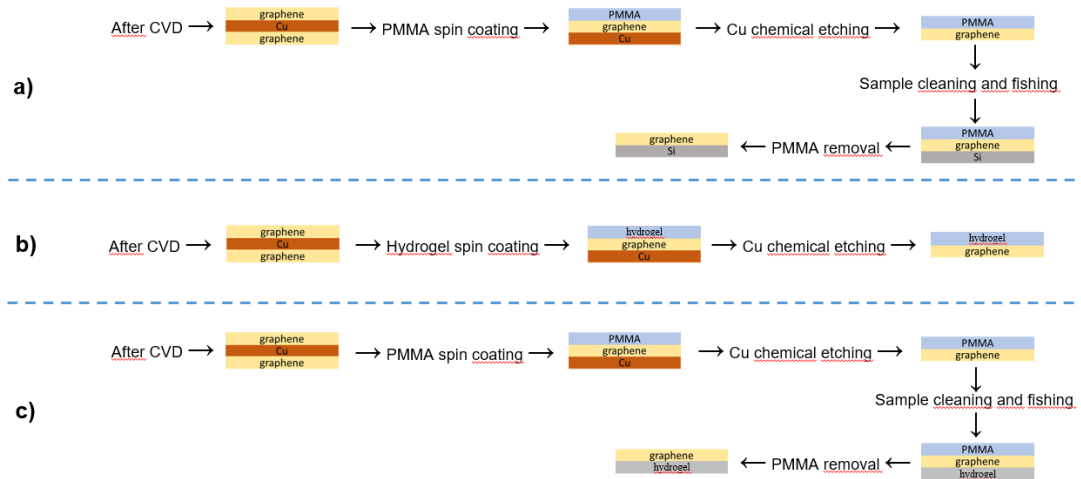
Figure 2.8: Different protocol overviews for graphene extraction. The extraction and transfer of graphene onto silicon wafer, in a), that was the basis of the one developed for the transfer onto hydrogel, in c), can be seen. In b) the transfer process was simplified, where hydrogel is placed directly on top of the Cu/graphene sample and then the Cu is etched after polymerization of the hydrogel.

2.2.2.C Graphene characterization

The characterization of graphene was performed on a Cu graphene stack, by using a LabRAM HR 800 Evolution Raman spectrophotometer (wavelength 200 nm - 1600 nm). The spectrophotometer has an internal laser of Helium-Neon (HeNe) with λ = 633 nm and an external diode laser of λ = 532 nm with a laser spot size of the magnitude of the wavelength. Data and spectrum aquisition are done in real-time using the machine's Horiba LabSpec 6 Spectroscopy Suite software. The laser intensity is set to 100%, using a grating of 600 gr/mm and a measurement duration of 10 seconds.

The process starts with a calibration step done with a Crystalline silicon (c-Si) piece, a material with a very sharp and defined peak at λ = 532 nm, and with very low backscattering noise. The peak obtained is used as a reference in the machine, before each measurement. The samples of graphene are analyzed as follows: the sample is loaded in the machine's optical microscope to inspect the surface. Regions and spots to analyze are chosen after usual inspection. With a magnification of 100x resolution, the spot is amplified and a measurement is taken. Three or four measurements are taken for each sample in different regions.

Measurements of Cu foil are done for reference. They present a higher backscattering of photons, creating more noise in the Raman spectrum. As such, treatment of the data is done, first using the machine software with an Intensity Correction System (ICS). Here the software automatically applies

the appropriate correction factor based on the active laser wavelength and diffraction grating pair. A subsequent treatment of the data was done using OriginPro 2016. A baseline correction and subsequent subtraction is performed using the Asymmetric least square (ALS) smoothing technique. An asymmetric factor between 0.002 and 0.01 is used imposing a threshold of 0.05% and smoothing factor of 5 and a smoothing through Adjacent-Averaging using a window with 5 points [22]. To colect the relevant peaks, for the study, the tool QuickPeaks was used with the local maximum method, using the full plot as region of interest, a y = 0 baseline and a minimum threshold of 5-20% filtering by height to avoid the residual noise, fig. 2.9.
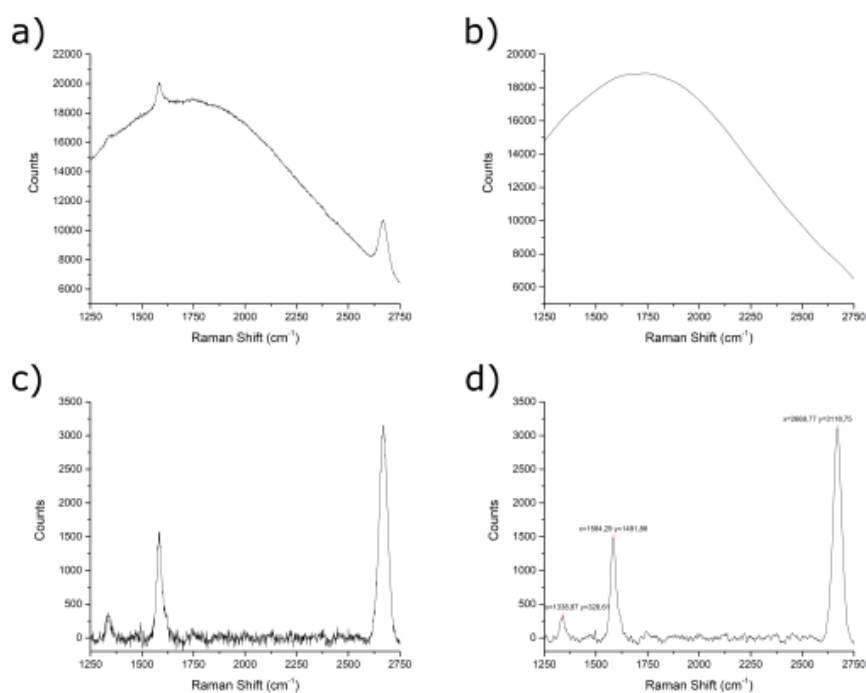
Figure 2.9: Processing steps of data from Raman spectrum of a Cu/graphene sample. In a) we see the raw data obtained with ICS correction. Using the ALS smoothing method (assymetric factor = 0.001, threshold = 0.05, smoothing factor = 5, iterations = 20) the baseline is obtained, b), then the baseline is substracted from the raw data to correct it, c), and a smoothing by adjacent-averaging (5 points) is done and peaks are obtained, d).

2.2.3   Assembly and characterization of the insert

After fabricating the hydrogel and preparing the graphene thin film, the graphene is fished onto the hydrogel surface.

Then, the stack is left to rest for at least 12h in a clean Petri dish, during which the hydrogel slowly dehydrates and the adhesion between the two layers is promoted. After bonding is complete, the PMMA is removed in an acetone bath and the resulting structure is re-hydrated with DI water.

2.2.3.A   Definition of shape and size

Having the insert designed to be inserted in the *cul-de-sac* of the eye, specifically to be used in vet-erinarian medicine, its dimensions had to be small enough to fit and be tolerated by the animal, while also having enough HA to diffuse onto the eye. Because of the dual layer nature of the insert and the graphene being transparent, a mark in the form of a cut corner was made so the correct positioning could be performed, with the hydrogel facing the sclera and the graphene layer facing the conjunctiva of the bottom eyelid.

Based on the eye dimensions for the dog, the inserts dimension was set at 10 mm length and 5 mm height, with a corner cut for the correct positioning. A curved cut in the underside was introduced when the *in-vivo* testing was being conducted, to improve biocompatibility. The cutters for the initial shape definition were prepared using metal blades mounted in Three dimensional (3D) printed supports. The design for the cutter supports was done using FreeCad software. The files were processed in Ultimaker Cura version 5.1.0 and 3D printed using a Ultimaker S3 printer with Polylactic acid (PLA) filament.

(a) FreeCad Design of cutters

(b) Ultimaker preview after slicing and optimizing for 3D print

(c) 3D printing process of the cutters

(d) 3D printed cutters with blades as-sembled
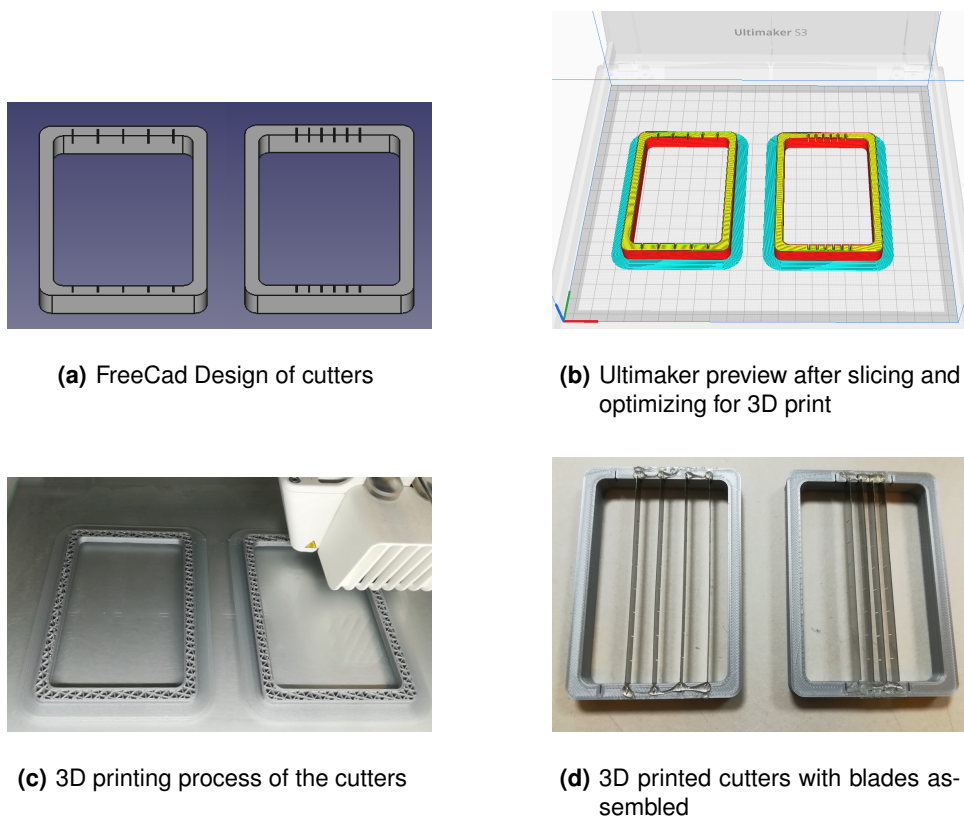
Figure 2.10: Stages of designing and fabricating the 3D printed cutters

After finishing the cutters, measurements of the distance between blades were made by taking im-ages and using ImageJ 1.53 for processing (Figure 2.11). The measured values are in Table 2.2.
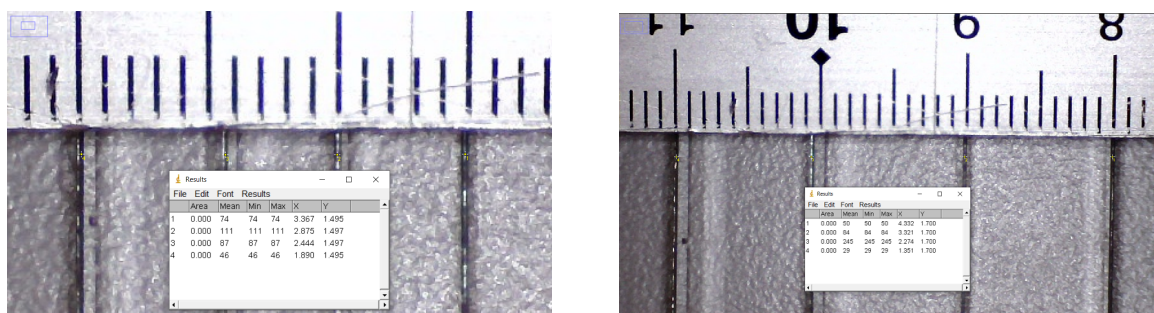
(a) Blade measurement of the 5 mm distance between blades

(b) Blade measurement of the 10 mm distance between blades

Figure 2.11: Measurements of the blades' inter distance for consistency and accuracy

Table 2.2: Measurements of the blades' distances in the cutters. The X position is defined by use of the software ImageJ and the distances are calculated by the difference of position. The % deviation is in regards to the set distance, either 5 or 10 mm

Cutter with 5 mm Blade distance			Cutter with 10 mm Blade distance		
Measurement	Distance (mm)	Relative deviation (%)	Measurement	Distance (mm)	Relative deviation (%)
1	4.92	1.6	1	10.11	1.1
2	4.31	13.8	2	10.47	4.7
3	5.54	10.8	3	9.23	7.7

For the corner and underside curved cuts (Figure 2.12), the design was made in Beam Studio software and the pieces cut using the laser cutter. In the former, the insert is placed on the rectangular hole and a blade follows the incision line and on the latter, the center of the curve is aligned with the bottom center of the insert, so it conforms to the shape of the *cul-de-sac*.

As the hydrogel in the dry form is brittle and fends to break, all the cuts are performed with the hydrogel in the hydrated form to prevent damage of the structures.

2.2.3.B   Determination of the concentration of Hyaluronic Acid

One of the key points in the biofunctionality of the device is the HA diffusion to the medium. For a given drug it is important that its amount is above the minimum effective concentration for treatment. For the particular case of the eye, optimum results of drug delivery would be effective in the pre-calculated daily dose that is based on the drug loading of eye drops.

A calibration curve of concentration of HA, Figure 3.4, was made with several measurements of known quantities of HA in a medium containing 0.2 M acetate buffer previously prepared and CTAB in 2 % NaOH solution, as explained previously in the turbidity assay. In this case 1 ml of HA mixed in DI water is added to 1 ml of acetate buffer and 2 ml of CTAB in 2 % NaOH solution and is left to incubate
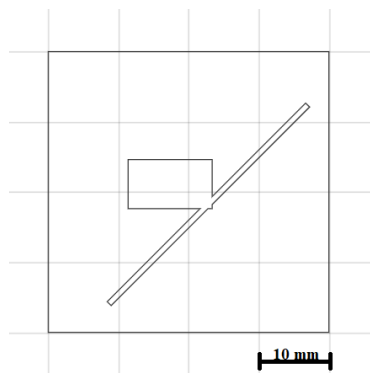
(a) Design of corner cutter for positioning of the insert

(b) Fabricated corner cutter for positioning of the insert
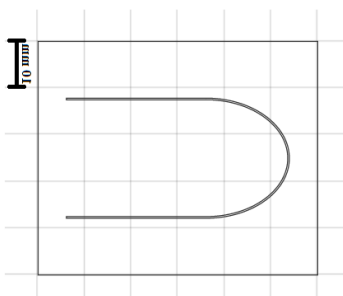
(c) Design of curved cutter to improve biocompatibility

(d) Fabricated curved cutter to improve biocompatibility

Figure 2.12: Designs and finalized cutters for corner and curved cuts

at 37 °C for 15 min.

Samples can then be analysed to measure the concentration of HA present and estimate how much is the insert diffusing into the medium.

All the weight measurements for the preparation of solutions presented below were performed in a Scientech SA 80 analytical balance, with a readability interval of d = 0.0001 g.

The acetate buffer used has a pH = 6 and is composed of a mixture of Sodium acetate (NaCH$_3$COO), Acetic acid (CH$_3$COOH) and Sodium Chloride (NaCl). To calculate the amount of acetic acid to be used, the Henderson–Hasselbalch equation was used:

$$pH = pK_a + \log_{10} \frac{[Base]}{[Acid]} \tag{2.1}$$

Knowing the final pH, the acetic acid pK$_a$ = 4.75 and that the final concentration of the buffer is set to 0.2 M of Sodium acetate, the equation gives:

$$6 = 4.75 + \log_{10}\frac{0.2}{[Acid]} <=> [Acid] = \frac{0.2}{10^{1.25}} <=> [Acetic\ acid] = 0.01125\ M \qquad (2.2)$$

To prepared the acetate buffer with final volume of 100 ml the steps were as follows:

- Add 60 ml of DI water to a 100 ml volumetric flask

- Add $0.2\ M \times 82.03\ g/mol \times 0.1\ L = 1.64\ g$ of Sodium acetate and mix.

- Add $0.01125\ M \times 60.05\ g/mol \times 0.1\ L = 0.0676\ g$ of Acetic acid (density is $1.05\ kg/l$), equivalent to to $0.064\ ml$, and mix.

- Add $0.15\ M \times 58.443\ g/mol \times 0.1\ L = 0.877\ g$ of sodium chloride and mix.

- Add DI water until completing 100 ml and homogenize.

- Add the solution to a 100 ml bottle, label it and store it for later use.

The CTAB in 2 % NaOH solution was prepared for a 100 ml final volume as follows:

- Add 60 ml of DI water to a 100 ml volumetric flask

- Add 2 g of Sodium Hydroxide (NaOH), and mix until dissolution.

- Add 2.5 g of CTAB, and mix until dissolution.

- Add DI water until completing 100 ml and homogenize.

- Add the solution to a 100 ml bottle, label it and store it for later use.

A trial was conducted to determine the amount of HA diffused into the medium, where two inserts from the same batch were fabricated with a loading of 1% w/v of HA and placed in two small laboratory bottles with 3 ml of Simulated Tear Fluid (STF). A magnet was placed inside each bottle and they were left in a magnetic stirrer at low RPM with the STF being replaced and stored every 24 h for 96 h. Afterwards, the mediums of each day were subject to the turbidity assay to determine the concentration of HA, see Table 3.3.

The STF solution was prepared for a 100 ml final volume as follows:

- In a 100 ml volumetric flask, 60 ml of ultra pure water was added using a syringe and filter with 0.2 μm nylon mesh.

- Add to the volumetric flask: 0.68 g of Sodium Chloride (NaCl), 0.22 g of Sodium Bicarbonate (NaCO$_3$), 0.008 g of Calcium chloride dihydrate (CaCl$_2$.2H$_2$O) and 0.14 g of Potassium chloride (KCL) and mix until dissolution.

- Add filtered ultra pure water until completing 100 ml, homogenize the solution by mixing.

- Add the solution to a 100 ml bottle, label it and store it for later use.

2.2.4 *In-vivo* testing of the insert

The patient used in the *in-vivo* trial was a female dog from a small Portuguese Podengo breed, castrated, 8 years old, very tame and docile. When the patient is first assessed there is an initial examination and before each of the three trials a quantitative assessment of conjunctivitis clinical signs was performed, in conjunction with baseline tests. It is then decided if the patient is healthy enough and within parameters to participate and continue with the trial. This study was performed in accordance with animal ethical requirements and it was approved by the Organ Responsible for Animal Welfare (Órgão Responsável pelo Bem-Estar dos Animais - ORBEA) of the Faculty of Veterinary Medicine, University of Lisboa, approval code 016/2022.

Three different types of inserts were used: an insert comprised solely of hydrogel loaded with 0.5 % HA, an insert of hydrogel loaded with 0.5 % HA and graphene layer, and an insert of hydrogel loaded with 0.5 % HA and graphene layer plus the PMMA layer used during transfer of the graphene, which wasn't removed.

Before placement of the insert, a drop of local anesthetic (Anestocil®, oxybuprocaine hydrochloride, Laboratório Edol, Carnaxide, Portugal) is placed in the eye that will receive the insert and the patient is left to rest until starting to take effect. While the patient is secured by the head, the insert is taken from the sterilized eppendorf with a sterile forceps and placed in the conjunctival *cul-de-sac*, as can be seen in Figure 2.13.
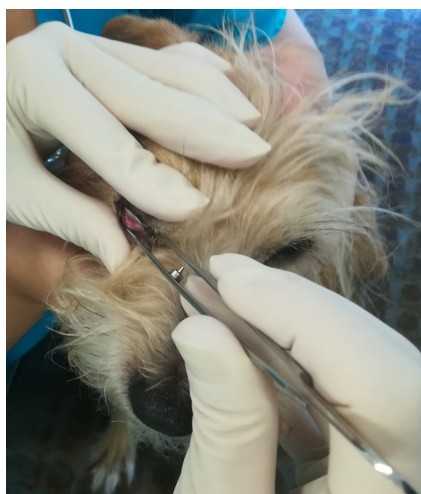
Figure 2.13: Placement of the insert into the right eye of the patient.

2.2.4.A   Sterilization protocol

To ensure the safety of the animal used in the *in-vivo* study, it was necessary to reduce the amounts of contaminants and to sterilize the inserts that were going to be used in the animal's eyes and also of the material used in their fabrication and manipulation.

After hydrogel polymerization, it is placed in boiling DI water for 15 min to remove unwanted non reacted monomers, that are toxic.

The transfer process of graphene onto the hydrogel was conducted in class 10 and class 100 clean room areas, ensuring a low amount of contaminants between the layers.

The cutters used to define the shape and size of the inserts were cleaned and disinfected with IPA prior to use.

The inserts were placed individually in eppendorfs with 2 ml STF solution that was made with ultra-pure water filtered with a 0.2 μm nylon mesh, as explained previously. Then the eppendorfs were subjected to 2h sterilization by radiation under UV light (velleman, 15 W) at close range 15 cm and in an enclosed setup.

The eppendorfs used for collection and preparation of samples, for example the Schirmer test strips, were autoclaved at 125 $^{\circ}$C for 18 min under 1.5 bar in a Sturdy SA-202 autoclave.

2.2.4.B   Patient evaluation and follow-up

An evaluation of basal state was initially performed by Dra Esmeralda Delgado. This initial examination of the eye assesses different aspects related to the health and physiognomy, such as symmetry, gross lesions and conformation. It should be performed from approximately 1 m away with good light conditions and minimal restrain of the head. Then in a darkened room the pupillary light reflexes and the anterior ocular segment are examined with a strong light and under magnification (Keeler PSL classic Portable Slit Lamp - magnification of 10x to 16x), see Figure 2.14(a). Everting the eyelids for examination, and vision testing such as the menace reflex and gently touching the lateral canthi, which normally stimulates a reflex blink, were also performed.

The baseline tests conducted were the Schirmer tear test (STT), using a STT strip with blue band Figure 2.14(b), and should give normal values in the range of 18.64 $\pm$ 4.47 mm/min to 23.90 $\pm$ 5.12 mm/min in the adult dog [43] and Intraocular pressure (IOP) measurement, using a TonoVet tonometer Figure 2.14(c), where values should be, for the normal dog, a mean of 19.0 mmHg with a range of 11 (5%) to 29 (95%) mmHg [44]. As said previously, in conjunction with these baseline tests, a quantitative assessment of conjunctivitis clinical signs was also done.

(a) Examination of the anterior ocular segment

(b) Schirmer tear test performed with a STT strip with blue band
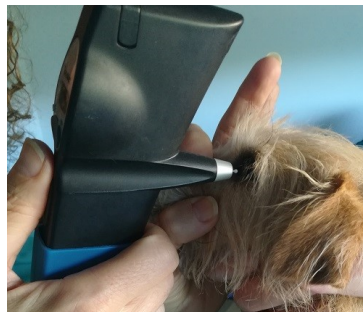
(c) Measurement of the intraocular pressure with a TonoVet tonometer

Figure 2.14: Initial ophthalmological examination of the patient

2.2.4.C   Insert biocompatibility

In order to understand if the insert was biocompatible its tolerance and biofunctionality were evaluated.

Insert tolerance was assessed by the continuous assessment of changes in measured parameters such as tear production and intraocular pressure and by the appreciation of the possible occurrence of eye injuries or discomfort associated with their presence in the conjunctival *cul-de-sac* using biomicroscopy. Clinical signs of conjunctivitis such as conjunctival hyperemia, chemosis, epiphora, the presence of ocular discharge, ocular pruritus and concomitant keratitis were evaluated, classifying them on a scale from 0 to 3 where 0 corresponded to normal and 3 to severe alteration. In addition, attention was paid to the presence of any possible corneal, scleral or conjunctival injury. This evaluation was performed using Slit Lamp Biomicroscopy (Kowa SL-15, Tokyo, Japan). Six hours after the insert placement at the level of the inferior conjunctival sac, the presence of the insert was verified, and a complete ophthalmological examination was performed.

The biofunctionality of the inserts was tested by evaluating the time elapsed between the moment of

placement and the time of either expulsion or collection, whenever they were still present at last recheck.

2.2.4.D   Follow up evaluations

Follow-up evaluations at the 6 h, 24 h, 48 h and 96 h of the various examinations were planned if the inserts would remain in the eye. Shortly after placement of the insert, 30 min to 1 h, a new STT was taken on the first and second trial and on the third after expulsion of the insert. IOP was also evaluated on the second trial after 2h. After each expulsion of the insert a new examination and a follow up examination a week after the third trial were performed.

3

Results and Discussion

Contents

The present chapter addresses the different trials, tests and experiments performed, summarizing and discussing the main results obtained. Some of the decisions made during the work are put into context in line with the results, changing the methods for thickness definition as one main example. Hydrogel fabrication and characterization, graphene growth, characterization and extraction and *in-vivo* testing of the insert are adressed in each section.

3.1   Hydrogel fabrication and characterization

With little to no information about the protocol of the preparation of this hydrogel in specific, initial trials were conducted to set the protocol conditions and to optimize them. At INESC MN there is a significant usage of spin-coating techniques to achieve thicknesses in the micrometer scale. As such, the first try was done with conditions commonly used for spin-coating of PDMS for the same thickness and SU-8 ([14, 45]).

Several tests were made to achieve a hydrogel.

The mixing of the reagents by hand in the proportions used in [13] to fabricate the hydrogel, resulted in a precursors solution with lower viscosity than that required for the spin-coating conditions imposed. To increase the viscosity of the solution, it was exposed to UV light in the UV-KUB 2. As example, in trial HT1 (table 3.1), the solution was placed in a Petri dish and exposed in the UV-KUB 2 for 1 min at 30 % power. After exposure, a viscosity increase was observed but still insufficient. Consequently another 10 seconds of UV exposure were imposed to the solution. The increased viscosity was satisfactory, but still a further 10 seconds exposure was performed, after which the solution became too viscous to spin-coat. The conditions for UV exposure were settled at 1 min 10 s for the next trial.

The various parameters and conditions from trial HT1 up to HT13 can be viewed in table 3.1.

Table 3.1: Quantities of the various reagents, parameters and conditions for the hydrogel fabrication trials made experimenting with different substrates, spin-coating protocols, and polymerization times.

	DI water (ml)	HEMA	EGDMA	MAA	PI (g)	Mix	Pre-curing (30 %)	Substrate	O$_2$ Plasma	Spin-coat	UV (30 %)
HT1	5.1757	4.673g	0.095g	0.094g	0.04857	15 min	1 min 1min10s 1min20s	-	-	-	-
HT2	5.1757	4.5788g	0.0788ml	0.0877ml	0.0505	5 min	1min10s	-	-	-	-
HT3	5. 176	4.3686g	0.0788ml	0.0877ml	0.0547	6 min	1min5s	Glass	-	P4	
HT4	5. 176	4.3686g	0.0788ml	0.0877ml	0.0547	-	-	-	-	-	-
HT5	5.176	4.369ml	0.079ml	0.088ml	0.055	5 min	1min5s	Glass	-	P4 P5 P4	2min 4min 5min
HT6	5.1757	4.3686ml	0.0788ml	0.0877ml	0.058	5 min	1min5s	Glass	- -	P5 PH1 P5	10min 15min 20min
HT7	5.1757	4.3686ml	0.0788ml	0.0877ml	0.0507	5 min	1min5s	Glass	-	PH2	15min
HT8	3.1054	2.6212ml	0.0473ml	0.0526ml	0.0312	5 min	1min5s	Glass	-	PH2	15min
HT9	3.105	2.6212ml	0.0473ml	0.0526ml	0.03	5 min	1min5s	Glass PMMA	-	PH3	8min
HT10	3.105	2.6212ml	0.0473ml	0.0526ml	0.03	5 min	1min	Glass PMMA	1min MED	PH4	-
HT11	2.5879	2.1843ml	0.0394ml	0.0438ml	0.0256	1min30s	1min	PMMA	-	S1	200 cycles 2s ON 1s OFF
HT12	2.588	2.184ml	0.039ml	0.044ml	0.030	1min30s	1min5s	Acetate sheet	1min MED	S1	200 cycles 2s ON 1s OFF
HT13	2.588	2.184ml	0.039ml	0.044ml	0.028	3 min	1min10s	Acetate sheet	1min MED	S2	200 cycles 2s ON 1s OFF

Starting from trial HT2 the mixing of reagents was made with the aid of a magnetic stirrer in a low power setting. The precursors solution was pre-cured for 1 min 10 s at 30% power, but it turned to a gel like consistency, too viscous to spin-coat. Since in the previous trial the pre-curing time of 1 min 10, it is assumed that this increase in viscosity resulted from inconsistencies of mass measurements in the analytical balance. The masses to be measured are close to the inferior limit of the balance, introducing errors in measurement. After this evaluation, the measurements of MAA and the EGDMA were done by volume using micro pipettes and tip.

For trial HT3 a pre-curing of 1 min 5 s was done, decreasing exposure time by 5 s. This decrease in exposure time and consequent decrease in viscosity allowed to evaluate the consistency of the solution and its appropriateness for spin-coating. A 30 min step of rest after the pre-curing step allows the solution to continue to slowly polymerize, which is not intended. Various lumps were found, which resulted in an uneven and unreproducible result. It was then necessary to reduce the resting time from the pre-curing to the spin-coating. Trial HT4 was discarded, since the hydrogel partially polymerised after mixing, possibly due to previous residues of hydrogel or excessive mixing, which acted as catalysts for the reaction.

Starting from trial HT5, all reagents except the PI that comes in powder form, were measured and added in volume. In this trial 3 samples from the same batch of solution were spin-coated in glass with different conditions. For the first sample, P4 was used with subsequent exposure to UV light for 2 min at 30% power. The second sample P5 and 5 min UV light exposure under the same conditions where imposed. Finally the third sample was spin-coated with P4, followed by 4 min of UV light exposure. The third sample had a resting time of 30 min before spin-coating and was slowly polymerizing into a hydrogel.

In trial HT6 three samples from the same batch were also used, this time starting with P5 and increasing the RPM from 500 to 1700 RPM for spin-coating. For the third sample, P5 was done again, after 20 min from the first P5 spin-coating. Even after 5 min UV exposure (HT6) the resulting solution had a sticky behaviour. To mitigate this an extra step of resting was implemented for 30 to 45 min. It was seen that 20 min rest between those two steps leads to a too viscous solution with lumps.

Since different conditions had been experimented, and the hydrogel seemed to become more consistent in fabrication, the first sample from trial HT5 and the three samples from HT6 were coated with a thin film of gold, for visual inspection and measurement of hydrogel thickness using a Scanning electron microscopy (SEM), Figure 3.1.

Although the surface could be visualized and some clues to its topography taken (fig. 3.1 - A), it was difficult to measure thicknesses of the samples (fig. 3.1 - B). The first sample from trial HT6 was placed sideways, to attempt to extract a measurement of the thickness, that was estimated using the machine software to be 39.54 μm. This estimation has an error associated with the capability of the operator to
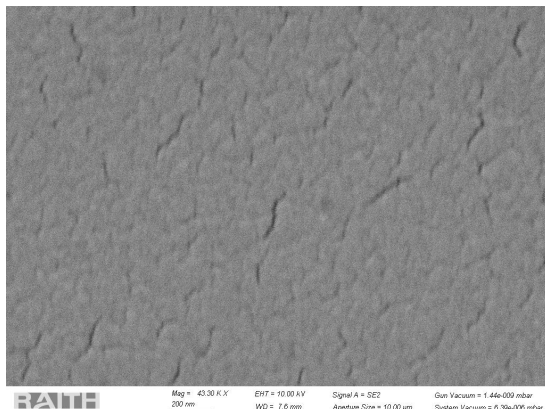
(a) Sample flat with hydrogel covered coated with a thin film of gold. The darker areas are flaws in the surface, probably due to the stresses induces in the gold filme by the hydrogel.
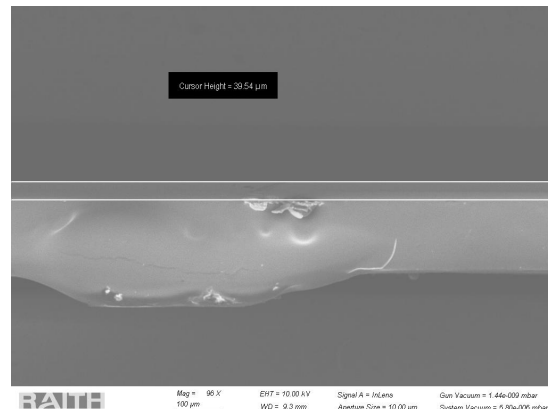
(b) Sample rotated at 90° annotated with lines at the interfaces glass-htdrogel and hydrogel-gold thin film/air for thickness measuremnets.

Figure 3.1: Images of scanning electron microscopy of the first sample from trial HT6. A 90° rotation for a side view enables the measurement of the thickness of each layer glass-hydrogel-gold/air

select the interface between the glass and the hydrogel based on the difference of intensity of gray. The thickness of the stack was found to be 193 μm. The thickness of the glass slides range from 0.13 to 0.17 mm given by the manufacturer, meaning that the hydrogel thickness ranges between 20 to 60 μm. Since the P5 imposed the lowest RPM during the spin-coating step for thickness definition, to achieve the thicknesses intended of 60 to 80 μm, the rotation speeds needed to be further decreased, to result in an increase in thickness of the hydrogel.

The decrease in RPM was set in HT7 and following. The program used was the PH2, that maintained the conditions for spreading the solution, but then decreased the spin speed from 1200 to 800 RPM. Excessive mixing speed however caused excessive amount of air bubbles to be trapped in the solution, and after spin-coating and UV curing, the resulting hydrogel had bubbles. From the knowledge gathered in the previous trials, the solution was divided in two batches, so that each half was pre-cured immediately before spin-coating (resting time = 10 seconds). However, the pre-curing step for 1 min 5 s at 30% power polymerized the hydrogel, coming out hard and brittle. This was maybe due to the high temperatures that the flow hood, where the UV-KUB 2 is, had a combination of temperature with lower volume of solution in the pre-curing, that speeds up the process of polymerization, since more energy reaches the monomers per volume unit. Trial HT8 was essentially a repetition of the previous, but it also had some problems with the air bubbles in the solution. More careful handling of the solution was taken into account, and also a step of sonication, that was employed in the later trials.

With the samples obtained from trials HT7 and HT8, testing was conducted to observe how the hydrogel would peel from the substrate by being in the trial HT7 hydrated, and in the trial HT8 in its dried

state. In its dried state it is not possible to peel it, since it doesn't have any malleability and since it is brittle, it starts to flake and break. After 1 hour and a half of being placed in water, the sample from HT7 was becoming softer and malleable, but it wasn't easy to peel. It was left until 5 hours of hydration had passed, and peeling was again attempted, but the hydrogel was adhered strongly to the glass substrate. Because of this, and also because it was observed in many of the spin-coating that the hydrogel would recede a fair bit from the edges of the glass, other substrates were taken into consideration, namely PMMA and the acetate sheet.

For trials HT9 and HT10, the difference between glass and PMMA as substrates was studied. In trial HT9 the substrates were used as is, and in trial HT10 by doing a surface treatment for 1 min in medium intensity of O_2 plasma, to increase the hydrophilicity of the surface and lowering the contact angle of the fluid. Without surface treatment the solution receding from the edges after spin-coat was much less on PMMA than on glass for trial HT9. In trial HT10, since it was experimented to decrease further the RPM in the thickness definition step, it became apparent that the machine couldn't handle such low speeds, maybe due to residue accumulation along the years, that imprints a resistance to the movement of the spinner, that gets overcome when imposing higher RPM. Already in trial HT9 it was observed that during the spreading step at 100 RPM the spinner didn't rotate, and only started when imposing 500 RPM during the thickness definition step. This meant that the results obtained from HT10 couldn't serve the purpose of comparing the substrate differences with surface treatment, but it was clear from HT9 that PMMA was the better option, with the advantage of being slightly malleable to potentially help during peeling.

Due to the necessity of using lower rotations to achieve higher flow thicknesses, and the inability to use the Laurell spin-coater for them, the setup was changed to a stepper motor controlled by an Arduino. For obtaining the calibration curve for the motor, it was set up with a Petri dish taped with double side tape to the top of the spinner of the motor, and 2 ml of water were added to simulate the weight it would have during operation. Then a series of inputs of increasing feed rate were given to the machine, and the data analysed, the result of which can be seen in Figure 3.2.

Trial HT11 was done to test the new low flow thickness conditions that could be imposed from the lower RPM and using PMMA without surface treatment to better compare to HT9. The resulting spin-coat was of high receding of the solution from the edges, that can be explained from variations that were being obtained from the pre-curing steps.

A new material for the substrate was then tested in trials HT12 and HT13, acetate sheet, already introducing from the onset of its usage the surface treatment with O2 plasma. The conditions that were changed from trial HT11 to HT12 were only the substrate and slight increase in pre-curing of 5 seconds and from HT12 to HT13 were only a slight increase in pre-curing of 5 seconds and a lowering of the thickness definition step from 20 to 10 seconds.
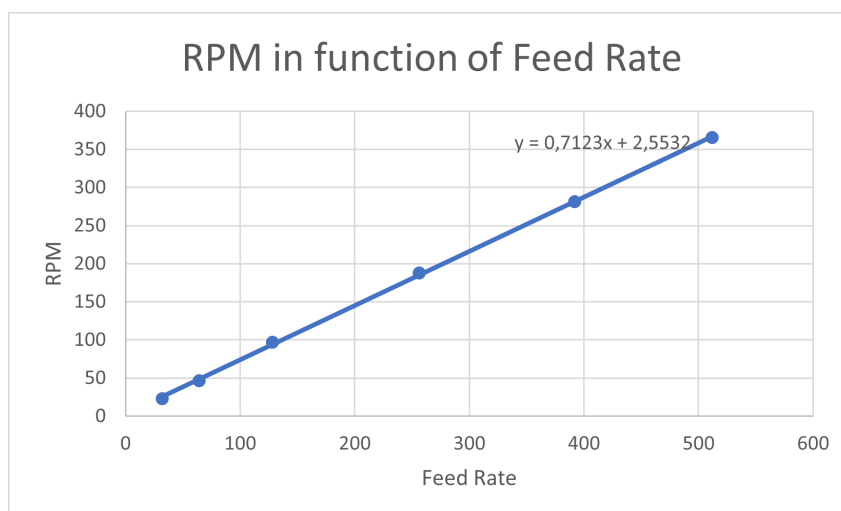
Figure 3.2: Calibration curve for the equivalence between input feed rate and output RPM in the stepper motor used. As seen, the correspondence is very linear, only changing slightly since terminal speed is not obtained immediately, as well as stoppage.

These two last trials were repeated two times from the same batch of solution, with receding of the solution on the substrate from the edges improved, although still present. It was observed that the second sample of each of the trials was thicker, due to accumulation of solution in the Petri dish and subsequently not room for it to properly escape during the spin-coat and also backtracking after the rotation of the motor stopped. During these two trials, due to an increase in thickness of the hydrogel a white opaque color appeared in the hydrogel after the UV exposure. When the hydrogel was left to dehydrate, the coloration disappeared and reappeared when hydrated again. This behavior is opposite of what was observed in [46], where the authors observe white colour when dehydrated, and transparent when hydrated, propably because of the use of different copolymers in conjunction with pHEMA. Nevertheless, when the copolymers of MAA is used [47], the same behaviour is observed.

A study was devised to test how to better handle the hydrogel after being polymerized, to peel, cut, and hydrate. The second sample from trial HT12 was used here, since it was thicker and would be better to handle. Four tests were conducted as follows:

1. Cut + peel + hydrate

2. Cut + hydrate + peel

3. Hydrate + cut + peel

4. Hydrate + peel + cut

The sample was first cut with a scissor in four pieces, and in each one was made one of the tests. A new surgical blade was used for the cuts and the peeling was made with standard laboratory tweezers.
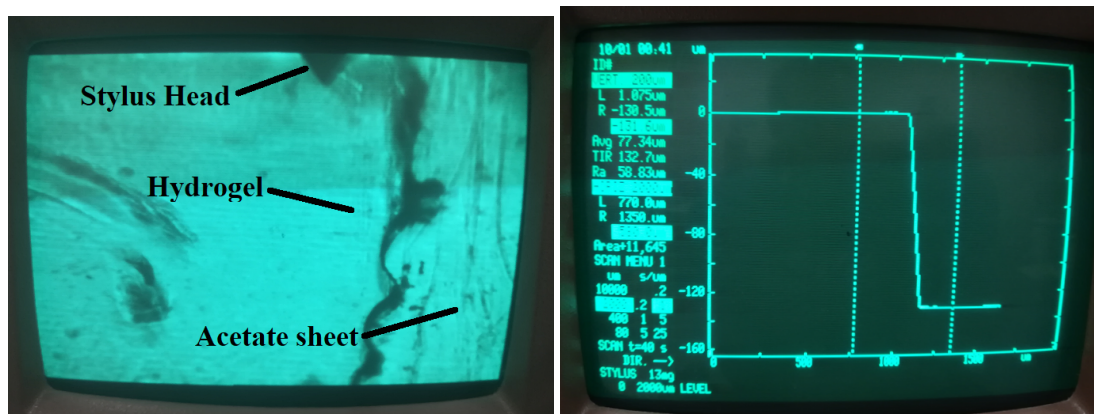
(a) The stylus head and the hydrogel-substrate interface can be seen, prior to taking a measurement in that region.

(b) The measurement taken, that reads 131 μm, is in fact more, since the stylus was left hanging in the air, maxed out. If the force of the stylus would be increased it would reach a maximum read of 200 μm.

Figure 3.3: Images taken from the display of the profilometer when performing measurements to try and determine the hydrogel thickness.

By starting with cut on the dry hydrogel, it results in the shattering of the hydrogel, since it is hard and brittle. As such, the results from tests 1 and 2 showed that the methodologies should be discarded. After 50 minutes of hydration, test 3 was conducted. Here the cutting step was performed easily, but the peeling was difficult as the hydrogel was adhering strongly to the substrate and when peeled would break. After, test 4 was carried in a way to guarantee the hydrogel not to break when peeling. It was also difficult to peel. A surgical blade was used to scrape the hydrogel slowly from the surface, but resulted in the blade damaging the hydrogel in several positions, making its surface irregular and damaged. Another peeling was performed in another piece cut from test 3 after 4 days of being immersed in water for hydration. This was done to evaluate if the adhesion to the substrate would decrease. Peeling was again difficult to achieve.

Profilometer measurements were done on a well defined edge between hydrogel and substrate without hydrogel. In the first test sample of HT12 was done to assess its thickness, which was found to be thicker than 131 μm, the maximum that the machine could read for the imposed settings, fig. 3.3. A second piece from the first test sample of HT12 was also cut and upon measuring returned an average of 78 μm thick, substantially less than the second sample, due to inhomogeneities of the solution.

Because a regular flat surface is more biocompatible and induce less stress, inflammation and strange body feeling to the eye, some testings were done by dipping the samples in different liquid reagents and study the adhesion between hydrogel and substrate. From trials HT12 and HT13, some pieces were cut and placed in Eppendorf tubes with IPA, acetone and ethanol for an amount of time.

An hydrated piece from the second sample of HT12 was placed with IPA and in a few minutes turned from white color into transparent. One piece of the first sample of the HT12 was placed in acetone which peeled after 1 hour. When removed to inspect, it curled and adhered to itself, making it not possible to unfold without damaging. Another piece of the first sample of HT12 was placed in the ethanol and a piece from HT13 was placed in acetone, this time for 2 minutes. Peeling was tested showing that the sample had lost almost all adhesion to the substrate and peeled easily. Nevertheless, manipulation was difficult as the sample was constantly adhering to itself. Even so, it is easier to manipulate the sample from HT12 after peeling. One of the key differences was noted to be the thickness between the samples, that also influenced the existence of the white color in the hydrogel. The thinner the sample, the less likely it is for the white color appear.

Another piece from HT12 was placed in ethanol. It started to feel by itself at 1 hour and a half. And broke easily with handling, which may be related with the ethanol affecting its structural integrity. This is also the case, when the samples are left in acetone for too long. Another explanation can be the rapid evaporation of ethanol, which may result in brittle spots interfacing with hydrated regions, causing internal stresses that will increase by manipulation. The piece immersed in IPA seem to have a similar behaviour than when hydrated in DI water.

For trials HT14 through HT16, the objective was to study if it was better and achievable to do a pre-curing step on the solution of hydrogel, then pipette a given volume onto the substrate, wait for it to spread evenly, reach the desired thickness and polymerize it. Trial HT15 was discarded, since after the pre-curing step, the resulting hydrogel became too viscous to be used in the study. This may have happened due to the LED lamp being hotter from usage increasinh the reaction rate. First, in trial of HT14, a sample was tested by pipetting 2 ml of pre-cured solution onto a 4x4 mm acetate sheet, and then exposing it to UV light to polymerize. On trial HT16, glass, PMMA and acetate sheet were tested side by side by pipetting 2 ml of the same solution onto each substrate. The viscosity obtained in the pre-cured solution made it hard to load in the pipette, resulting in different volumes placed onto each substrate. The various parameters and conditions from trial HT14 up to HT16 can be viewed in table 3.2.

Table 3.2: Quantities of the various reagents, parameters and conditions for the hydrogel fabrication trials made in different substrates by directly pipetting the precursors solution on the surface.

	DI water (ml)	HEMA	EGDMA	MAA	PI (g)	Mix	Pre-curing (30 %)	Substrate	Pipetted	UV (30 %)
HT14	2.588	2.184	0.039	0.044	0.025	4 min	1min5s	Acetate sheet	2 ml	200 cycles 2s ON 1s OFF
HT15	2.588	2.184	0.039	0.044	0.025	5 min	1min5s	-	-	-
HT16	3.1054	2.6212	0.0474	0.0526	0.033	3 min	1min	Glass PMMA Acetate sheet	2 ml	200 cycles 2s ON 1s OFF

One of the main limitations that were occurring so far in the fabrication steps of the hydrogel were the inconsistencies derived from the pre-curing. It was highly dependent on temperature of the room, temperature of the flow hood, of the LED light and the energy per volume of solution. Due to this, it was

decided that this step needed to be eliminated from the process, but since the hydrogel solution is very fluid, the spin-coating and pipetting directly onto the substrate couldn't work. The solution to the issue that was pursued was casting, and a mold was developed.

The idea behind the first iteration of the mold (V1), was to have a squared block of acrylic (PMMA) 5 mm thick, milled to have a pocket with 2.8 mm depth and 40 mm width that fits a square of 2 mm thick acrylic with width of 39 mm, the bottom lid. Then, by having a rim milled at a depth of 0.5 mm to fit another acrylic square with width of 44 mm that would serve as a top lid, the difference in height between the two would be the thickness of the hydrogel, 300 μm (fig. 2.2). In trial HT17, more than trying the new process for defining the size of the hydrogel, the sonication step was introduced to aid in the removal of air bubbles trapped in the prepolymer solution after mixing, and for the polymerization step an attempt was made to cure the hydrogel by placing it in the oven. The objective was to see if the difference in process would give a different result in the transparency of the hydrogel. The oven curing was stopped after 1 hour and a half, since it was still liquid, and upon research, [48] show that it would take closer to 36 hours of curing in the oven. Since the transparency is not critical, the insert won't be covering the pupil of the eye, this method was dismissed in regards to the faster times achieved in curing by UV light.

Despite the transparency not being critical, according to [46], as previously mentioned, the hydrogel should have a white color when dehydrated (xerogel) and should turn optically transparent in hydrated form. Trying to dismiss improper protocol for fabrication, in trial HT18 less power of exposure was used (10 % = 3.5 mW/cm^2) and also less time of exposure, since there could be an over exposure occurring. Time of exposure of 5 and 8 min continuous exposure (ON) were tried. The first came out transparent but still viscous and a bit fluid and the second was already slightly white and was left to rest for the next day. The next day it was hard, brittle and transparent, since it was dehydrated. Upon hydration it was peeled and started showing white color again.

From trial HT19 forward, the exposure cycle was modified to 8 cycles of 2 min ON and 30 s OFF at 30 % power, increasing the time for continuous exposure, while allowing the LED to rest, preserving it. In this trial, two samples were cast on the same mold V1, each with half the prepolymer solution. Some design flaws started to show, a lot of time was needed between castings, because the hydrogel had to be removed and residues cleaned. Also, since there was nothing securing the bottom lid, it tended to float in the solution, making the thickness of the hydrogel unpredictable. To avoid this problem, a new mold (V2) was fabricated. This time the mold was completely done with use of the laser cutter from a piece of square acrylic with 2 mm thickness, Figures 2.3(a) and 2.3(b). Has explained previously, the main piece has a hole cut through and it is closed of by using a bottom lid secured with Kapton tape and a top lid, with the thickness definition done by use of spacers.

Trial HT20 was done with the mold V2 and 320 μm spacers, but the after the first curing was completed the hydrogel had leaked through the bottom, so it was removed and secured properly again, and

a new curing was done with the remaining prepolymer solution. Since the top lid had also been secured with Kapton tape, that crossed on top of the solution, it absorbed much of the energy from the exposure and didn't cure the hydrogel fully.

On trial HT21 it was studied if the alternative protocol in fig. 2.8(b) was viable. For this, a sample of copper/graphene was placed inside the mold V2 and the prepolymer solution was poured on top, the top lid was placed with the spacers providing the correct thickness and the hydrogel was cured. On two attempts, when pulling the top lid out of the mold the hydrogel would come out adhered to it, but the copper/graphene sample would peel right off, and it was decided to abandon this alternative.

From trial HT22 forward, the hydrogel formulation was to be tested with the addition of the HA, based on the work from Maulvi2017 [13]. To calculate how much HA should be added to the prepolymer solution, it was first calculated how much HA was in the previous referenced work.

$$Hydrogel\ ring:\ 6\ mm\ inner\ diameter\ ;\ 8\ mm\ outer\ diameter\ ;\ 0.08\ mm\ thick \tag{3.1}$$

$$Volume_{ring}\ =\ \frac{\pi * 0.08}{4} * (8^2 - 6^2)\ =\ 1.75929\ mm^3 = 0.00175929\ ml \tag{3.2}$$

$$Present\ work\ insert:\ 10\ mm\ widht\ ;\ 5\ mm\ height\ ;\ 0.3\ mm\ thick \tag{3.3}$$

$$Volume_{insert}\ =\ 10 * 5 * 0.3\ =\ 15\ mm^3\ =\ 0.015\ ml \tag{3.4}$$

$$Ratio\ of\ volumes:\ \frac{Volume_{insert}}{Volume_{ring}}\ =\ \frac{0.015}{0.00175929}\ =\ 8.5262 \tag{3.5}$$

There are 80 μg of HA loaded in each ring, of which 20 % gets retained and is not diffused, corresponding to 16 μg. Assuming that the hydrogel from the present work will behave similarly, it will also retain 20 %:

$$Retained\ amount\ of\ HA\ in\ one\ insert\ =\ 16 * 8.5262\ =\ 136.42\ \mu g \tag{3.6}$$

For a total volume of 5 ml, the amount of HA that should be retained is:

$$Ratio\ between\ total\ volume\ and\ insert\ volume\ =\ \frac{5}{0.015}\ =\ 333.333 \tag{3.7}$$

$$Amount\ of\ HA\ =\ 136.42*333.333\ =\ 45473\ \mu g\ =\ 45.473\ mg \tag{3.8}$$

On top of the retained HA, the insert should also be able to diffuse to the environment, so loading an additional 80 μg per insert gives:

$$HA\ to\ be\ delivered\ =\ 80*333.333\ =\ 26.667\ mg \tag{3.9}$$

$$Total_{HA}\ =\ 45.473 + 26.667\ =\ 72.14\ mg \tag{3.10}$$

During trial HT22, HA was first used, and upon mixing the powder in the prepolymer solution it created lumps of powder that wouldn't dissolve, and wouldn't mix. Upon research, it was found that it was an expected occurrence, and that it takes a long time for HA to dissolve in water, as it is continuously absorbing water and creating a gel like barrier, [49, 50]. It was advised to use cold water or high energy mixers, and since the latter produces a high amount of bubbles trapped inside the hydrogel, the first option was opted. It also felt like it was a very concentrated load of HA added into the solution, making it very viscous. Since different studies mention usage of HA concentration up to 1 % w/v [13, 16], and the syringes used during eye surgeries have 1.8 to 2.2 % w/v, the amount of HA was adjusted for 0.5 %, 1 %, and 2 % w/v to be tested.

Trial HT23 was done with 2 % w/v of HA, but the beaker containing the solution fell during the sonication step, contaminating the sample, and had to be discarded. In trial HT24 the solution was made with 0.5 % w/v of HA, and two samples were tried from the same batch, now using the mold V3, that had a slot for the spacers, preventing them from floating around, and had the addition of buckles to secure the top lid in place, instead of floating in the solution (figs. 2.3(c) and 2.3(d)). After curing, one of the samples was peeled right away and the other after 15h to let it dehydrate and stabilize. The peeling didn't show much difference, mainly because the addition of HA makes it harder for the hydrogel to dehydrate, retaining the water for longer. It was not easy to peel, it had to be done with patience and if pulled with some force to try and detach it, the hydrogel would stretch a bit and deform.

The spacing in mold V3 was very tight, and made it difficult to insert the spacers, even more so after usage, with the slots becoming filled with hydrogel residues, so a new mold V4 was devised with bigger slots (figs. 2.3(e) and 2.3(f)). It was used starting in trial HT25 that replicated the conditions from HT23. After mixing and sonication, the solution had lumps and bubbles, so it was put in the fridge to rest until next day. The lumps were still present, and after trying to mix again it didn't help, seemed to be maxed out on the capacity to dissolve the HA. It could also be due to the order of mixing the reagents,

namely the PI, since it formed a lot of lumps with the HA, and wouldn't dissolve completely either. The solution was cured, but had no consistency to it and would break very easily. It seems that because the PI didn't dissolve, the polymerization reaction didn't occur correctly and the polymer chains weren't built and crosslinked as they should. Trial HT26 was a repetition of HT25, but now mixing first the prepolymer reagents without DI water and the HA with DI water separately and then adding them together while mixing. When added it immediately starts to form lumps and after curing the hydrogel isn't well made.

For trial HT27, the mixing of HA with DI water was replaced by using 2 ml of 2.2 % w/v HA in a commercially prepared syringe for use during eye surgery. This way it would eliminate user error from the preparation of the HA step, but the result was the same, forming lumps.

Trials HT28 and HT29 were made with respectively 0.5 % w/v of HA and 1 % w/v of HA, for the purposes of making an estimation of HA diffusion by detection via the turbidity assay. In HT28, everything went fine during the mixing, but after the sonication step it gained a significant lump. It was put in the fridge to see if it would dissolve, but it wouldn't, so the HT29 trial, that had no problems during fabrication, and was reserved in the fridge during a week and a half, was used to fabricate an hydrogel, that was boiled in 6 ml of DI water to remove unwanted monomers, and cut to shape with the fabricated cutters.

Then, two pieces (insert 1 and insert 2) were used for the diffusion testing. Each one was placed inside a small lab beaker with 3 ml of STF solution and stirred with a magnetic stirrer at low setting and room temperature. Each 24 h, the different samples of solution were collected and new solution was added. In the end they were analysed, resulting in the following data, Table 3.3. Since in the first trial the results were very low and close to zero, a second trial was made, using the same sample collection, since it was only used 1 ml per sample, and it had 3 ml. The second trial had close results, with some small values, but so close to zero, that it is hard to know if it is really detecting HA, or simply is within the error of the machine. This may mean that the hydrogel insert is not diffusing HA, or it is diffusing much less quantities than the machine has resolution to measure. The calibration curve that was made, fig. 3.4, used the concentrations of HA of 0.5; 1; 25; 50; 200; 400; 500; 650 μg/ml. Being 0.5 μg/ml of HA the lowest amount, when by the measurements of other works [16], the hydrogel diffuses in the first two hours a burst of up to 8 μg/h and then has a release of around 416 ng/h, adding up to around 25 μg in 24 h for the 3 ml of solution, making 8.33 μg/ml, which may be in the lower extremity of the capacity for the spectrophotometer to read. It would make more sense for the results to be reversed, showing some small values in the earlier times of collection and zero closer to the 96 h of diffusion, but it shows the opposite, that can indicate a higher probability for a false reading.

The various parameters and conditions from trial HT17 up to HT29 can be viewed in table 3.4.

Table 3.3: Turbidity as measured at λ = 640 nm for different timestamps of diffusion of HA from two inserts in STF

Time of collection	First trial		Second trial	
	Insert 1	**Insert 2**	**Insert 1**	**Insert 2**
96 h	0.003	0.000	0.000	0.000
65.5 h	0.005	0.001	0.002	0.003
Baseline	0.003		0.000	
48 h	0.000	0.003	0.000	0.000
24 h	0.000	0.000	0.000	0.000
Baseline	0.002		-0.004	

Table 3.4: Quantities of the various reagents, parameters and conditions for the hydrogel fabrication trials made experimenting with different mold configurations and HA concentrations. Trials HT22 and HT27 were discarded after UV exposure in a Petri dish cover, and trial HT23 was contaminated and was also disposed of.

	DI water (ml)	HEMA	EGDMA	MAA	PI (g)	HA	Mix	Sonication	Substrate	Mold	UV (30 %)
HT17	5.1757	4.3686	0.0788	0.0877	0.05	-	5 min	15 min	PMMA	V1	200 cycles 2s ON 1s OFF / Oven 70 $^\circ$C 1h30
HT18	5.1757	4.3686	0.0788	0.0877	0.05	-	4 min	10 min	PMMA	V1	5 min 10% / 8 min 10%
HT19	2.588	2.184	0.039	0.044	0.030	-	3 min	-	PMMA	V1	8 cycles 2min ON 30s OFF
HT20	2.588	2.184	0.039	0.044	0.030	-	3 min	-	PMMA	V2	8 cycles 2min ON 30s OFF
HT21	1.294	1.092	0.0195	0.022	0.015	-	3 min	-	Graphene	V2	8 cycles 2min ON 30s OFF
HT22	2.588	2.184	0.039	0.044	0.031	0.0756g	10 min	-	-	-	8 cycles 2min ON 30s OFF
HT23	2.588	2.184	0.039	0.044	0.031	0.052g	20 min	-	-	-	-
HT24	2.588	2.184	0.039	0.044	0.030	0.01294g	10 min	15 min	PMMA	V3	8 cycles 2min ON 30s OFF
HT25	2.588	2.184	0.039	0.044	0.031	0.053g	30 min	30 min	PMMA	V4	8 cycles 2min ON 30s OFF
HT26	2.588	2.184	0.039	0.044	0.031	0.0516g	10 min	-	PMMA	V4	8 cycles 2min ON 30s OFF
HT27	2	1.712	0.031	0.036	0.0195	2.2% w/v	10 min	-	-	-	-
HT28	2.588	2.184	0.039	0.044	0.025	0.01294g	5 min	15 min	PMMA	V4	8 cycles 2min ON 30s OFF
HT29	2.588	2.184	0.039	0.044	0.031	0.02588g	5 min	-	PMMA	V4	8 cycles 2min ON 30s OFF

3.2 Graphene growth, characterization and extraction

To grow graphene in a substrate, there are a lot of parameters to take into account, such as temperature, heating ramps and cooling ramps, pressure, growth time, annealing time and gas flows. The recipe tested as basis was from [22], using a copper foil with 99.999 % purity, due to known results in growing quality graphene from literature. The higher the purity, the higher the chance for low defects in the graphene grown, but it also depends on other factors, like the grain size of the Cu, reason why the annealing step takes an important role. Before placing the Cu substrate in the furnace, on top of the heater, it is necessary to cut it to size from a roll, and then making it as flat as possible and wrinkle free. To flatten it, a roller was used, placing the Cu sample between two cleanroom papers and passing the roller with some pressure from different angles. Also, the surface may be cleaned with IPA and DI water if needed. Some other steps for sample preparation, as adding an oxidation layer on the back side may be done to reduce graphene nucleation density there [28].

During the first trials the machine and its functioning was being tested, and seemed to behave well
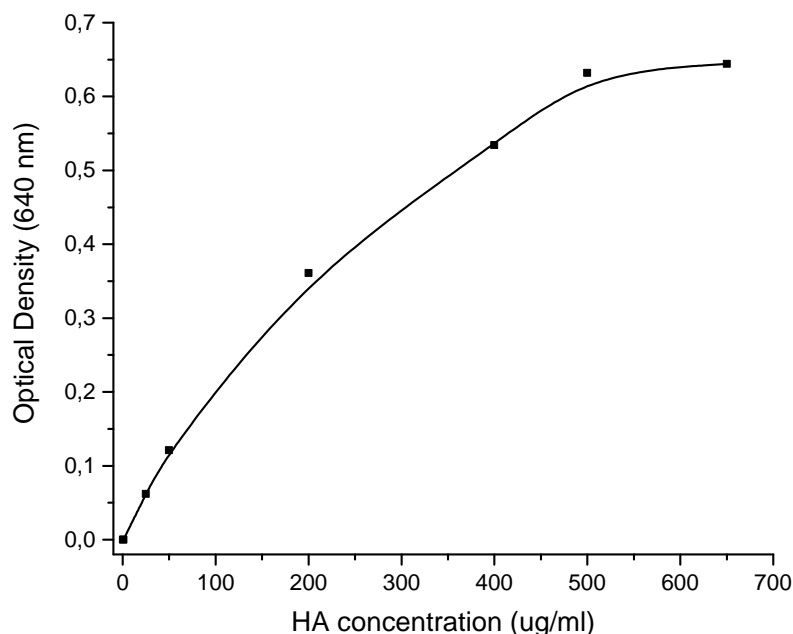
Figure 3.4: Relation between the turbidity as measured at $\lambda = 640$ nm and the hyaluronic acid concentration.

in accordance to the recipes used, but it had issues with the copper substrate sublimating. After a while the heater would plateau at a temperature that was below the set temperature, no matter how much time passed. The recipe initially used can be seen in listing A.1.

The main commands "TUNE HTTC", "TUNE PCON", "FLOW", "HEAT", and "WAIT" are used, respectively, to set how the response to the difference between set and current temperature and is made and what is the max power output, to set the pressure inside the vacuum chamber, to control the flow of gasses, to set the target temperature and heating and cooling ramps, and to make sure the machine doesn't advance for the next step before a set of conditions is met.

Throughout the trials for growth, one of the main difficulties present was the control of temperature. The machine varies wildly its readings from the thermocouple depending on the position it is placed on top of the heater, and just randomly changes from possibly how the machine is behaving in the moment to the different external and internal conditions. In some trials the temperature was set with the HEAT command for 850 °C but couldn't pass over 790 °C, while if it was tried a few days later it would manage to go above. Many trials were invested in trying to make the machine work and understand what would be necessary to correct the disparity in reached and target temperatures, including disassembly, cleaning, and replacement of the thermocouple. While it seemed to help on occasion when these changes were made, the vast majority of the trials fell short of being able to reach annealing temperatures and subsequently the graphene growth step.

In the trials in which the target temperature was successfully reached, the copper substrate tended to sublimate in varying degrees. Sometimes as soon as the temperature for annealing was reached, other times it would hold until the introduction of CH_4 and then would rapidly sublimate, since the presence of the CH_4 starts the reactions for graphene growth that create miniature eruptions by combination of the CH_4 with H_2 in the substrate's surface.

In Figure 3.5, are shown two graphs, one in which the max set temperature was equal to 825 °C, which the CVD machine had no problem in delivering, and then one in which the temperature was set even higher at 900 °C, but still the machine cannot surpass 810 °C. In previous trials to the second one shown, the CVD was already showing problems with reaching the set 825 °C, reason why it was increased to 900 °C, trying to set a higher difference to force the CVD to achieve higher temperatures.
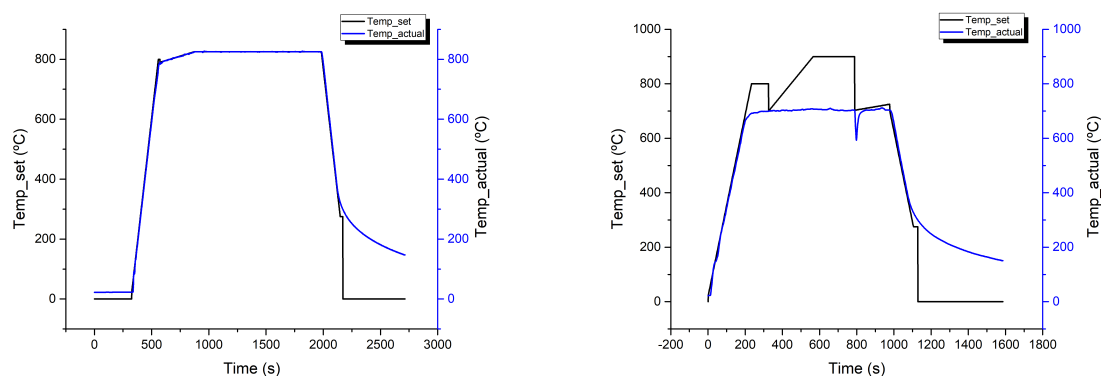
(a) Graph of set and actual temperatures for trial A1. The temperatures were equivalent and there was no issue. Max set T = 825 °C

(b) Graph of set and actual temperatures for trial Ttest1. Despite having a higher Max set T = 900 °C, the actual T didn't pass 810 °C.

Figure 3.5: Comparison of two trials that show the disparity in achieving the set temperature in the CVD.

Only much later, in fact towards the end of this work, it was found the issue resided in the TUNE HTTC commands, that had a parameter to cut the max output power to the heater to a certain percentage. A new test, fig. 3.6 was made where a set T = 1000 °C with a ramp of 500 °C/min is the target for the heater at each step, while the TUNE HTTC parameters are set with an increase of 10 % more max power each time. A waiting time of 180 s between steps is placed with the command WAIT.

In the test data it can be seen that the only limiting variable is the TUNE HTTC command, that caps the output power the heater can receive. By changing those parameters in the recipes, knowing the corresponding temperature cap, would ensure that the temperature target would be reached, without risking a high spike power pull from the machine, that would overshoot the temperature.

The fourth trial made, used a Si wafer between the heater and the substrate to provide shielding from the current passing through the heater, that could be passing through the substrate and causing
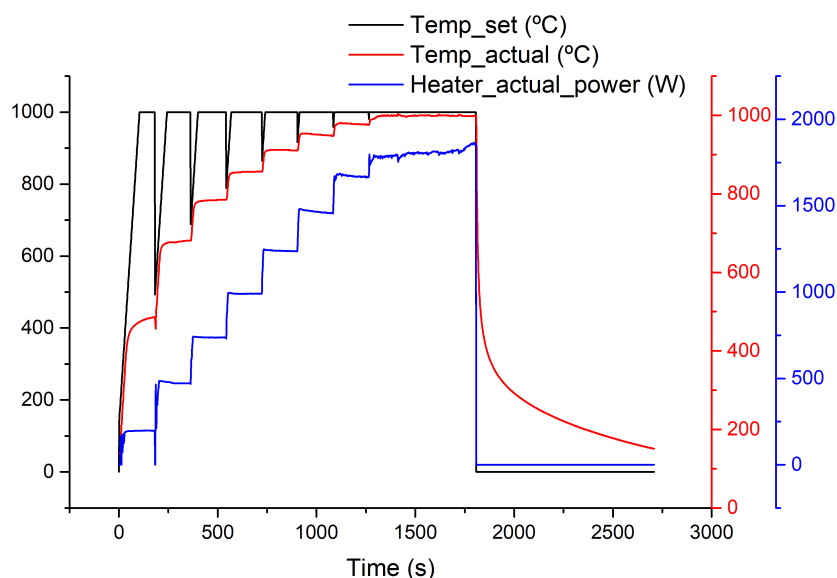
Figure 3.6: Testing made with increasing max output power percentage (10 % per step) imposed by TUNE HTTC commands. Set T = 1000 °C with 500 °C ramp.

it to sublimate. The trial seemed to went well, but then during the cool down phase, the wafer couldn't hold the thermal stresses and broke. It also had the peculiar effect of turning the copper substrate in a grayish metallic color. The sample was observed by X-ray difractometry, but the spikes corresponding to the "metalization" couldn't be identified, fig. 3.7.

After the previous trial, the heater started failing to reach the target temperatures and plateauing. A cleaning of the thermocouple was made as previously mentioned and a test was conducted to see if the heater could reach the temperature of 950 °C, which it did. In alternative, it was thought of using a disk of thick copper as a holder for the copper foil substrate, to prevent it from sublimating, by also shielding it from the direct current that may pass through the substrate, while allowing for thermal conductivity. A 2 inch disk was cut in the milling machine, the edges sanded to eliminate sharp points that could serve as initiators for sublimation and it was tested with the same 950 °C target. The results can be seen in fig. 3.8. The actual temperature of the heater rose on par with the set temperature and surpassed the sublimation point of copper for this low pressures of 20 mbar. Since it was a thick disk, a lot of material deposited itself back down on all exposed parts inside the furnace, and the CVD machine had to be partially disassemble to be cleaned, including the thermocouple again, that was lightly sanded with a grit 3000 sandpaper.

The graphene characterization was done by Raman spectroscopy and the data analysis used the ALS and the adjacent-averaging smoothing techniques. From the parameters discussed in chapter 2, the threshold value was the one that sometimes was altered, to conform the baseline produced closer

(a) Sample of Si wafer with copper foil after being taken out from the CDV machine, broken due to rapid cooling.
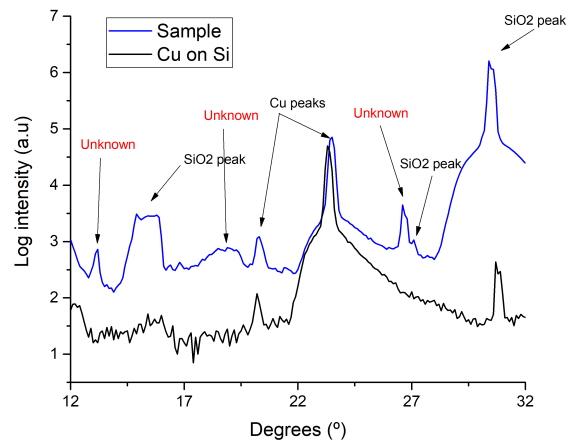
(b) Result from X-ray difractometry on the sample and on copper foil on top of c-Si

Figure 3.7: A trial made to study if the sublimation of copper would be lessened by using a Si wafer resulted in an unknown transformation of the copper foil and breaking of the wafer.

to what felt correct, varying from 0.02 to 0.07. Despite the alterations that using different values in the parameters produce, the baseline will affect the points in a manner that is proportional, meaning that the ratios of the peaks shouldn't be altered, but may help to evidence better a smaller peak, that would otherwise be buried in noise. The ratios are calculated based on the average intensity of the peaks from the different measurements, and in the cases were the D peak was absent, it was considered to be 0 for the averaging, table 3.5.

Table 3.5: Raman spectrum average measurements of graphene over copper after baseline subtraction with asymmetric least square and adjacent-averaging smoothing techniques applied. In sample A.5, there is no data for the 2D peak, because there was an operator error only discovered while processing the data. When setting the range of the spectra [1150-2650 cm^{-1}], instead of [1250-2750 cm^{-1}], while the 2D peak is in the [2670-2700 cm^{-1}] area.

Sample	D peak	G peak	2D peak	I(D/G)	I(2D/G)
A.2	1338,87	1587,39 ± 2,68	2670,67 ± 0,78	0,073 ± 0,127	2,31 ± 0,19
A.3	1345,25	1580,67 ± 0,89	2691,35 ± 3,56	0,036 ± 0,063	1,79 ± 1,60
A.4	1339,35 ± 4,61	1583,11 ± 2,89	2675,74 ± 8,72	0,85 ± 0,82	1,62 ± 0,91
A.5	1344,37 ± 0,92	1598,86 ± 7,31	-	1,14 ± 0,52	-

Peak centroid	1341,96 ± 3,32	1587,51 ± 8,06	2679,26 ± 10,78

Several trials of graphene extraction and transfer were conducted to understand the process and mechanize it for the transfer onto hydrogel. Samples from previous work in graphene growth [22] were used as training, table 3.6.
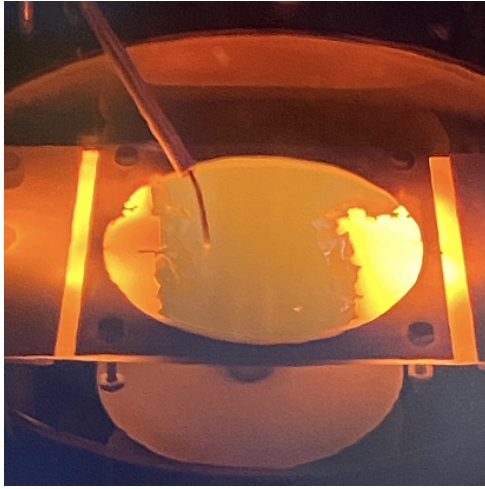
(a) Temperature testing done with a thick copper disk. In the image is possible to see the disk sublimating.

(b) Disk after being taken out from the CVD furnace. The sides that were facing the eletrodes of the heater are sublimated and melted.
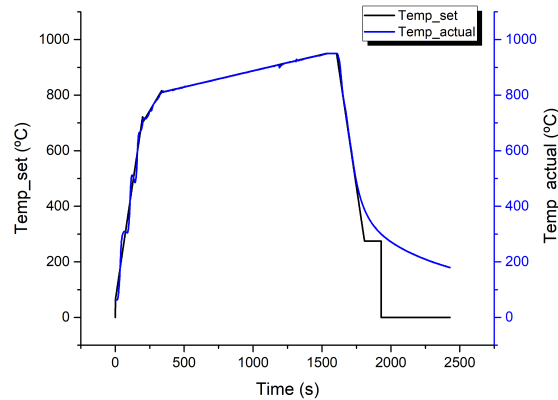
(c) Graph with set and actual temperatures during the temperature test with copper disk. Max temperature reached was 950 °C.

Figure 3.8: Copper disk that was to be used as a support for copper foil substrate gets sublimated during a temperature test of the machine.

The first two trials, following a slightly modified protocol from appendix D, and done with sample Plasma 25 (twice, the sample was cut in half) resulted in failures due to externalities. In the first trial the PMMA coating was done in the SVG track, then the Cu was etched with $FeCl_3.6H_2O$ solution. After 1 h of etching at 37 °C, there was still a lot of copper spots left that weren't etched. The sample was phished with a glass slide and placed in DI water until next day. Then it was placed in the etching solution again for 30 min at 37 °C and 15 min at 40 °C. More of the copper was etched, but there was

Table 3.6: Raman spectrum measurements of graphene over copper after the asymmetric least square fitting of peak centroids and heights [22].

Sample	D peak	G peak	2D peak	I(D/G)	I(2D/G)
Plasma 25	1350.06 ± 0.39	1595.85 ± 0.65	2693.15 ± 1.66	2.17 ± 0.11	0.15 ± 0.03
PPBN4	1346.52 ± 7.55	1590.24 ± 4.59	2689.10 ± 18.67	2.26 ± 1.54	1.02 ± 1.09
PPBN6	1350.67 ± 7.68	1614.55 ± 1.16	2694.18 ± 16.12	1.94 ± 0.81	0.25 ± 0.12
PPNC1	1356.38 ± 17.19	1579.27 ± 4.98	2667.68 ± 15.43	0.44 ± 0.85	2.00 ± 0.92

Peak centroid	$1350,90 \pm 3,53$	$1591,92 \pm 14,49$	$2683,67 \pm 11,99$

still copper that wouldn't etch. What is more likely is that during the growing of graphene it also grew on the backside of the sample and was acting as a protective layer in those spots. A new trial was started and the etching of the copper this time removed the entirety of the copper substrate, leaving just the graphene/PMMA layers on the sample. During the cleaning steps the sample was inside a beaker with DI water, the sample folded onto itself and against the wall of the beaker. It was not possible to unfold it, due to adhesion forces and when forced to separate, the sample started to tear.

The third trial used sample PPBN4 (a small piece was cut and the rest stored for later uses). After the spin-coating of PMMA, the sample was etched for 1 h 50 min at 38 °C, but some copper residues were still in the sample. It was left in DI water overnight followed by cleaning steps. The sample was transferred onto a piece of Si wafer, and left to dry over the weekend. The sample was then placed in an acetone bath for 2 h and 1 h in ethyl acetate bath to remove the PMMA layer.

In the fourth trial, another two pieces of sample PPBN4 were used. When doing the transfer step of graphene/PMMA stack onto Si, the membrane stack trapped water between the c-Si and the graphene, that resulted in the membrane wrinkling after drying. In these trials, compressed air was used to force the air bubbles to be removed from the interface between layers, while also helping to flatten the graphene/PMMA against the c-Si. It is a fickle process to do, since the graphene and PMMA layers are quite fragile, and very easily tear, which did happen to one of the samples. The samples were then left to dry overnight, and the following day the PMMA layer was removed in acetone bath for 1 h and ethyl acetate bath for 2 h.

After the trial HT21 done previously failed to produce a adhesion between graphene and hydrogel, a trial for extraction and transfer of graphene onto hydrogel was made using this same hydrogel. Sample PPBN6 (table 3.6) was used as the graphene donor. The steps for extraction of the graphene are the ones described in appendix D and the transfer is done by placing the hydrogel on top of the glass slide and use it to phish the graphene/PMMA stack from a beaker with DI water. After phishing and letting the sample rest for 30 min on top of the glass slide, it was placed in a beaker with DI water, but as soon as it entered the water, the graphene began peeling from the hydrogel, so it was instead left on the glass slide overnight to see if the adhesion would improve. The following day, the glass slide with the stack of hydrogel/graphene/PMMA was placed in a beaker and slowly water was added to rehydrate

the hydrogel. No signs of peeling from the graphene were observed. After rehydration and no peeling, it was placed in an acetone bath to remove the PMMA and observe the effects that it might have on the hydrogels structure and on the adhesion between graphene and hydrogel. The hydrogel showed no signs of damage after 30 min in the acetone bath and the graphene exhibited no peeling. The sample was placed in a Petri dish with DI water.

After the successful extraction and transfer onto hydrogel from the previous trial, the hydrogel from HT24 (table 3.4) and the copper/graphene sample PPNC1 (table 3.6) were used. Following the extraction protocol (appendix D, both the extraction and the transfer were done with success. After transferring the graphene/PMMA stack onto the hydrogel, it was left overnight to improve the bonding while dehydrating slightly, since the presence of HA doesn't let the hydrogel dehydrated easily, fig. 3.9.
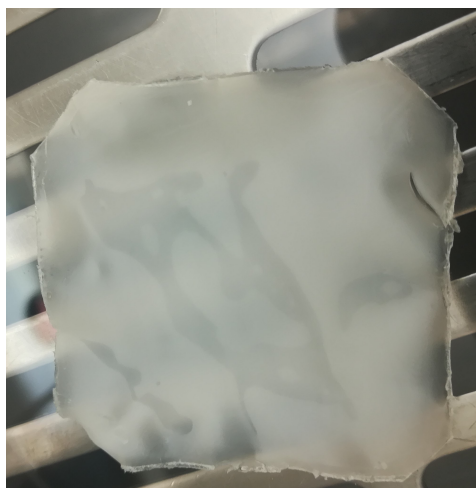
(a) Hydrogel before transfer process. Notice the white color of the hydrogel.
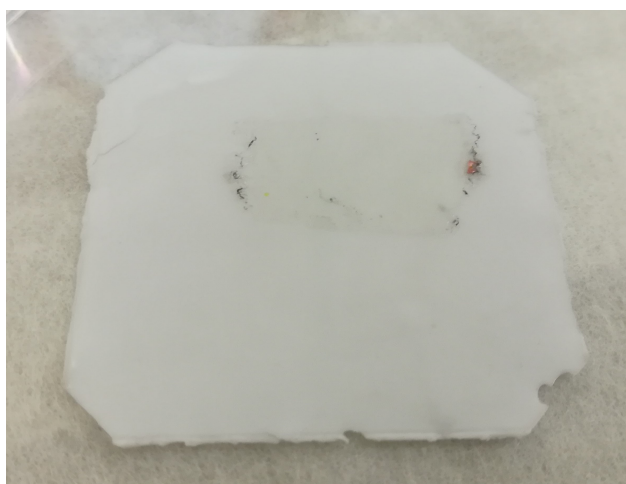
(b) After conclusion of the transfer process, but before bonding of the layers. Some copper residues still present.

Figure 3.9: Hydrogel from trial HT24, before and after having the graphene/PMMA transferred. Some copper residues are still present on the edges, but they were discarded during the cutting steps.

3.3 *In-Vivo* testing of the insert

For the purposes of the *in-vivo* testing of the insert that was mentioned in the previous section, sterilization and biocompatibility (comprising tolerance and biofunctionality) are needed to be taken into account. To do this, the insert was boiled in 6 ml of DI water to remove unreacted monomers and cut with the help of the fabricated cutters, previously disinfected.

A few cuts of the hydrogel were left with the stack hydrogel/graphene/PMMA, while others were placed in an acetone bath to remove the PMMA film. Since the graphene doesn't cover the total area
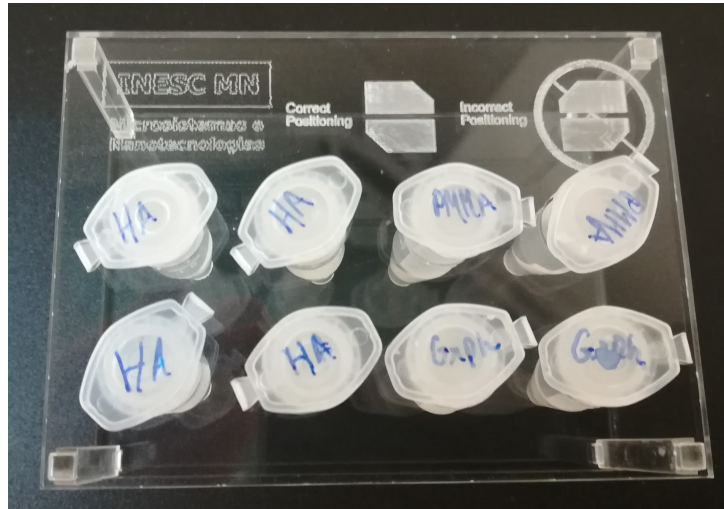
Figure 3.10: Eppendorf tubes supporter with instructions on how to place the inserts correctly in the eye and labelled tubes with the different insert types.

of hydrogel, a few pieces were also cut without graphene or PMMA. They were placed in labelled Eppendorf tubes with 2 ml of STF solution (fig. 3.10) and sterilized by radiation under UV light for 2 h at close range 15 cm, and in an enclosed setup. Eppendorf tubes for the collection of samples were sterilized in autoclave at 125 °C for 18 min under 1.5 bar.

Before testing the inserts in vivo, a request was submitted to the ethics commission ("Comissão de Ética para a Investigação e Ensino"), and the owner of the patient gave written informed consent to participate. The commission's positive decision and the informed consent can be found in appendix E.

Three trials were devised, one using only the hydrogel with 0.5 % w/v HA, another with the addition of the graphene layer and a third with the PMMA layer onto the graphene . This last trial is possible due to the PMMA being a material that is biocompatible, being also one of the first materials used in ocular lens fabrication [11, 14].

On the day of the first trial, the patient's basal state was fully evaluated by Dra. Esmeralda Delgado, intended to assess different aspects related to the health and physiology of the patient. In conjunction with the baseline tests, a quantitative assessment of conjunctivitis clinical signs was also done, and its results can be seen in table 3.7. The health of the patient was deemed to be enough to proceed with the trial. The right eye was chosen for testing, with the left eye being used as control.

Before placement of the insert, a drop of local anesthetic was placed in the eye and 5 min were waited for it to take effect. Then the placement was conducted with a sterilized tweezers, and required two persons. One to place the insert and another to hold the patient's head. Initially it took some attempts at correctly placing the insert in the *cul-de-sac*, since it tended to be pushed out to the middle of the eye. Once in the correct position, it stayed there and the patient was not showing signs of irritation or discomfort. After 5 min of placing the insert and looking for signs of discomfort, another STT was

taken, giving 12 mm/min, somewhat below the normal range, but it was done in a short period of time following the initial STT test, so it was expected that the tear fluid of the eye hadn't been restored fully.

After 2 h of placing the insert, an assessment of the tolerance and reaction of the patient was done and no signs of lesion, discomfort or irritation were seen. Around 1 h before the 6 h mark for new evaluation, in a routine check of the patient, it was observed that the insert had been expelled from the eye. A new examination of the patient state was conducted, with particular attention given to clinical signs of conjunctivitis and lesions. No additional effects were seen in the eye due to the presence of the hydrogel (table 3.7).

Table 3.7: Results of the ophthalmic examination in Trial number 1, in which the insert was expelled before the 6h time point, including STT, IOP values and conjunctivitis signs evaluation. The insert used had only hydrogel with 0.5% HA. A STT done 5 min after placement of the insert gave 12 mm/min. O.D. and O.S. means oculus dexter and oculus sinestra, respectively.

(a)

Before insert placement	
Date	17/10/2022
Type of insert	Hydrogel with HA
Eye	Right
STT (mm/min)	20 O.D. & 17 O.S.
IOP (mmHg)	15 O.D. & 15 O.S.

(b)

Quantitative assessment of conjunctivitis clinical signs				
	Before placement		Insert expelled (6h)	
	O.D.	O.S.	O.D.	O.S.
Conjunctival hyperemia	1	1	1	1
Chemosis	1	1	1	1
Epiphora	0	0	0	0
Pruritus	0	0	0	0
Ocular discharge	0	0	0	0
Concomitant keratitis	0	0	0	0
Total Score	2	2	2	2

Trial number 2 was done the following day. The same extended examination was performed and the patient was deemed to be healthy enough to proceed. A new trial was conducted on the opposite eye (left eye) with an insert of hydrogel/graphene, using this time the right eye as control. Shortly after placement of the insert, around 1 h, a new STT was taken wielding a result of 15 mm/min and an IOP after 2 h with a result of 15 mmHg, all within normal values. The insert was expelled before the 6 h evaluation mark, and a new examination of clinical signs was conducted. The results can be seen in table 3.8.

Table 3.8: *In-vivo* trial number 2, with the insert expelled before the 6h evaluation. The insert used is complete with graphene and hydrogel with 0.5% HA. A STT after 1h gave 15 mm/min and IOP after 2h was 15 mmHg for the O.S.. O.D. and O.S. means oculus dexter and oculus sinestra, respectively.

(a)

Before insert placement	
Date	18/10/2022
Type of insert	Hydrogel/Graphene
Eye	Left
STT (mm/min)	18 O.D. & 17 O.S.
IOP (mmHg)	18 O.D. & 18 O.S.

(b)

Quantitative assessment of conjunctivitis clinical signs				
	Before placement		Insert expelled (6h)	
	O.D.	O.S.	O.D.	O.S.
Conjunctival hyperemia	1	1	1	1
Chemosis	1	1	1	1
Epiphora	0	0	0	0
Pruritus	0	0	0	0
Ocular discharge	0	0	0	0
Concomitant keratitis	0	0	0	0
Total Score	2	2	2	2

Two days after the second trial, the third trial was conducted. The patient was again examined, and this time it showed some signs of conjunctival hyperemia and chemosis, and it was noticed that from trial 2 to 3, that the rim of the left eye's eyelid had gained a small whitish spot. This may be the result of some microscopic copper residues left trapped in the graphene layer, that weren't completely etched and removed in the cleaning steps. Apart from that, the patient exhibithed no signs of discomfort and the STT and IOP tests were within normal range. The patient received permission to continue with the last trial. Here, an insert of hydrogel/graphene/PMMA was placed on the right eye, but this time, to try and improve biofunctionality, a new cutter was devised to do a circular cut on the basis of the insert, to conform better to the shape of the *cul-de-sac* (fig. 3.11). The cut was done and the insert placed in the eye. the insert was expelled, after around 1 h 15 min. An examination was done that showed the presence of the same clinical signs (table 3.9), with a follow up examination a week after the third trial concluding that the white spot in the eyelid had disappeared and the conjunctivitis clinical signs had returned to basal values.
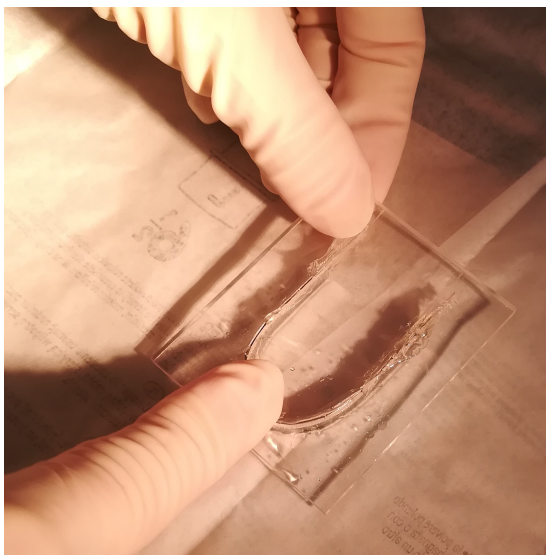
(a) Cutting of the hydrogel in sterile conditions

(b) Comparison between inserts that are uncut (bottom) and cut (top) with a round bottom

Figure 3.11: Cutting and comparison between the shapes of inserts. The round bottom is meant to improve bio-functionality

Table 3.9: *In-vivo* trial number 3, with the insert expelled after 1h15min. The insert used did not have the PMMA layer removed after the transfer process, meaning that is has PMMA, graphene and hydrogel with 0.5% HA. A STT performed in the O.D. after expulsion of the insert gave 17 mm/min. O.D. and O.S. means oculus dexter and oculus sinestra, respectively.

(a)

Before insert placement	
Date	20/10/2022
Type of insert	With PMMA
Eye	Right
STT (mm/min)	17 O.D. & 17 O.S.
IOP (mmHg)	20 O.D. & 14 O.S.

(b)

Quantitative assessment of conjunctivitis clinical signs				
	Before placement		Insert expelled (1h15min)	
	O.D.	O.S.	O.D.	O.S.
Conjunctival hyperemia	2	2	2	2
Chemosis	2	2	2	2
Epiphora	0	0	0	0
Pruritus	0	0	0	0
Ocular discharge	0	0	0	0
Concomitant keratitis	0	0	0	0
Total Score	4	4	4	4

4

Conclusions and future work

Contents

4.1 Conclusions

The main objective of the work was to fabricate a device to treat the chronic dry eye syndrome, by placing it non invasively in the eye, allowing for a slow and sustained release of HA in time at an effective dose. The majority of the work focused the fabrication of the hydrogel, in the optimization of the conditions for which the result would be an hydrogel film of ideal dimensions and drug loading. Different methods of achieving the hydrogel thickness were studied namely: spin-coating, direct pipetting and casting, as were different amounts of HA concentration and different approaches for being able to mix the components. The best results were obtained for casting spreading technique, concentration 0.5% w/v and by mixing the HEMA, MAA, EGDMA, and PI separately from the HA with DI water, joining them after. The testing of the release profiles of the device were insufficient to draw conclusions and more testings needs to be performed in the future. Cutters were designed and fabricated to define the shape of the device, allowing for better uniformity between different samples. Better blade stability will help preventing wobbling of the blades during cutting in the future.

A novel approach of using graphene as an added layer for water and drug retention was a specific objective, involving the graphene growth, extraction and characterization. Tests for process temperature, cleanings and thermocouple replacement were conducted to enhance the yield of graphene growth. In particular it was found that the parameters that control the looping feedback of the heater, were restricting the power output at which the heater could reach for an increase of process temperature. Also, the temperature of the heater surface was seen to vary significantly depending on the positioning of the sample relative to its center and to the connector of the electrodes that delivers the current and voltage to the heater. The inconsistencies in temperature readings and set points made it more difficult to control the sublimation processes of the copper.

The insert was tested *in-vivo*, to conclude on its biocompatibility, including assessment of both tolerance and biofunctionality. A volunteer patient was found and three trials conducted. The devices remained in the eye for at least 1 h 15 min in trial 3 up to an indeterminate amount out time below 6 h, for trials 1 and 2. Although none reached the programmed 6 h hour evaluation after placement, the development showed promising results. The presence of the insert was well tolerated by the patient, but the residence time was considered low, meaning that the insert biofunctionality still needs to be improved.

4.2 Future work

Several points addressed in this work cam be further improved, namely:

- The peeling of the polymerized hydrogel from the substrate can be further investigated, by different

surface treatments or by optimization of solvents and time of application of the solvent, facilitating the process and inducing less internal stresses to the type of hydrogel.

- The study of the loading of the HA cause systematized, as well the release profiles through diffusion in the medium.

- The introduction of the HA in the formulation of the prepolymer solution alters its properties, namely increasing the viscosity, so there is no need for the pre-curing step, which introduced high uncertainty in the viscous behaviours of the hydrogel, hence allowing for the spin-coating to be pursued and optimized.

- An improved setup for the turbidity assay should also be employed, to improve the resolution in the range of the expected diffusion concentration of HA.

- Since only towards the end of this work, the real underlying causes that compromised the graphene growth in terms of operation of the Aixtron BlackMagic 2" CVD machine were found, the quality and coverage of the graphene on the Cu substrate could be better optimized. Better growth may mean that the graphene film is more stable, allows for better etching of the Cu and bonds with hydrogel in a faster and stronger fashion.

- To improve biofunctionality of the device, it is necessary to either better adapt its shape to the conjunctival *cul-de-sac* or to abandon this location, exploring alternatives with other shapes and locations, such as hemispheric corneal contact lenses, as long as the microfluidic device is transparent enough to allow for a non blurred vision.

- The thickness of the device should be decreased, trying to maintain sufficient structural integrity to endure manipulation, while attempting to achieve optical transparency.

Bibliography

[1] A. R. Thode and R. A. Latkany, "Current and Emerging Therapeutic Strategies for the Treatment of Meibomian Gland Dysfunction (MGD)." *Drugs*, vol. 75, no. 11, pp. 1177–1185, jul 2015.

[2] A. Shaharudin and Z. Aziz, "Effectiveness of hyaluronic acid and its derivatives on chronic wounds: a systematic review," *Journal of Wound Care*, vol. 25, no. 10, pp. 585–592, sep 2016. [Online]. Available: https://www.magonlinelibrary.com/doi/abs/10.12968/jowc.2016.25.10.585

[3] H. D. Perry, R. Solomon, E. D. Donnenfeld, A. R. Perry, J. R. Wittpenn, H. E. Greenman, and H. E. Savage, "Evaluation of topical cyclosporine for the treatment of dry eye disease." *Archives of ophthalmology (Chicago, Ill. : 1960)*, vol. 126, no. 8, pp. 1046–1050, aug 2008.

[4] V. J. Drew, C.-L. Tseng, J. Seghatchian, and T. Burnouf, "Reflections on Dry Eye Syndrome Treatment: Therapeutic Role of Blood Products." *Frontiers in medicine*, vol. 5, p. 33, 2018.

[5] A. R. C. Celebi, C. Ulusoy, and G. E. Mirza, "The efficacy of autologous serum eye drops for severe dry eye syndrome: a randomized double-blind crossover study." *Graefe's archive for clinical and experimental ophthalmology = Albrecht von Graefes Archiv fur klinische und experimentelle Ophthalmologie*, vol. 252, no. 4, pp. 619–626, apr 2014.

[6] R. Toyos, W. McGill, and D. Briscoe, "Intense pulsed light treatment for dry eye disease due to meibomian gland dysfunction; a 3-year retrospective study." *Photomedicine and laser surgery*, vol. 33, no. 1, pp. 41–46, jan 2015.

[7] J. V. Greiner, "A single LipiFlow® Thermal Pulsation System treatment improves meibomian gland function and reduces dry eye symptoms for 9 months." *Current eye research*, vol. 37, no. 4, pp. 272–278, apr 2012.

[8] N. J. Friedman, K. Butron, N. Robledo, J. Loudin, S. N. Baba, and A. Chayet, "A nonrandomized, open-label study to evaluate the effect of nasal stimulation on tear production in subjects with dry eye disease." *Clinical ophthalmology (Auckland, N.Z.)*, vol. 10, pp. 795–804, 2016.

[9] T. Romero-Rangel, P. Stavrou, J. Cotter, P. Rosenthal, S. Baltatzis, and C. S. Foster, "Gas-permeable scleral contact lens therapy in ocular surface disease." *American journal of ophthalmology*, vol. 130, no. 1, pp. 25–32, jul 2000.

[10] M. B. McDonald, H. Sheha, S. Tighe, S. B. Janik, F. W. Bowden, A. R. Chokshi, M. A. Singer, S. Nanda, M. A. Qazi, D. Dierker, A. T. Shupe, and B. J. McMurren, "Treatment outcomes in the DRy Eye Amniotic Membrane (DREAM) study." *Clinical ophthalmology (Auckland, N.Z.)*, vol. 12, pp. 677–681, 2018.

[11] H. P. Filipe, J. Henriques, P. Reis, P. C. Silva, M. J. Quadrado, and A. P. Serro, "Contact lenses as drug controlled release systems: A narrative review," *Revista Brasileira de Oftalmologia*, vol. 75, no. 3, pp. 241–247, 2016.

[12] F. A. Maulvi, T. G. Soni, and D. O. Shah, "Extended Release of Timolol from Ethyl Cellulose Microparticles Laden Hydrogel Contact Lenses," *Open Pharmaceutical Sciences Journal*, vol. 2, no. 1, pp. 1–12, apr 2015.

[13] F. A. Maulvi, A. A. Shaikh, D. H. Lakdawala, A. R. Desai, M. M. Pandya, S. S. Singhania, R. J. Vaidya, K. M. Ranch, B. A. Vyas, and D. O. Shah, "Design and optimization of a novel implantation technology in contact lenses for the treatment of dry eye syndrome: In vitro and in vivo evaluation," *Acta Biomaterialia*, vol. 53, pp. 211–221, 2017. [Online]. Available: http://dx.doi.org/10.1016/j.actbio.2017.01.063

[14] C. S. A. Musgrave and F. Fang, "Contact Lens Materials: A Materials Science Perspective," *Materials*, vol. 12, no. 2, jan 2019. [Online]. Available: /pmc/articles/PMC6356913//pmc/articles/PMC6356913/?report=abstracthttps://www.ncbi.nlm.nih.gov/pmc/articles/PMC6356913/

[15] W. H. Chang, P. Y. Liu, M. H. Lin, C. J. Lu, H. Y. Chou, C. Y. Nian, Y. T. Jiang, and Y. H. H. Hsu, "Applications of Hyaluronic Acid in Ophthalmology and Contact Lenses," *Molecules*, vol. 26, no. 9, 2021. [Online]. Available: /pmc/articles/PMC8123179//pmc/articles/PMC8123179/?report=abstracthttps://www.ncbi.nlm.nih.gov/pmc/articles/PMC8123179/

[16] F. A. Maulvi, T. G. Soni, and D. O. Shah, "Extended release of hyaluronic acid from hydrogel contact lenses for dry eye syndrome," *Journal of Biomaterials Science, Polymer Edition*, vol. 26, no. 15, pp. 1035–1050, 2015.

[17] D. Nguyen, A. Hui, A. Weeks, M. Heynen, E. Joyce, H. Sheardown, and L. Jones, "Release of Ciprofloxacin-HCl and Dexamethasone Phosphate by Hyaluronic Acid Containing Silicone Polymers," *Materials (Basel, Switzerland)*, vol. 5, no. 4, pp. 684–698, apr 2012. [Online]. Available: https://pubmed.ncbi.nlm.nih.gov/28817003/

[18] J. M. Song, J. H. Im, J. H. Kang, and D. J. Kang, "A simple method for hyaluronic acid quantification in culture broth," *Carbohydrate Polymers*, vol. 78, no. 3, pp. 633–634, oct 2009.

[19] I. Palacio, G. Otero-Irurueta, C. Alonso, J. I. Martínez, E. López-Elvira, I. Muñoz-Ochando, H. J. Salavagione, M. F. López, M. García-Hernández, J. Méndez, G. J. Ellis, and J. A. Martín-Gago, "Chemistry below graphene: Decoupling epitaxial graphene from metals by potential-controlled electrochemical oxidation," *Carbon*, vol. 129, pp. 837–846, apr 2018.

[20] J. Y. Choi, "Graphene transfer: A stamp for all substrates," *Nature Nanotechnology*, vol. 8, no. 5, pp. 311–312, 2013. [Online]. Available: http://dx.doi.org/10.1038/nnano.2013.74

[21] J. Kang, D. Shin, S. Bae, and B. H. Hong, "Graphene transfer: key for applications," *Nanoscale*, vol. 4, pp. 5527–5537, 2012. [Online]. Available: http://dx.doi.org/10.1039/C2NR31317K

[22] P. Alexandre de Carvalho Gomes and I. Superior Técnico, "Optimization of Graphene Deposition Conditions by Chemical Vapour Deposition: Impact of Temperature," Ph.D. dissertation, Instituto Superior Técnico, 2017. [Online]. Available: https://fenix.tecnico.ulisboa.pt/downloadFile/563345090415854/main.pdf

[23] X. Li, L. Colombo, and R. S. Ruoff, "Synthesis of Graphene Films on Copper Foils by Chemical Vapor Deposition," *Advanced Materials*, vol. 28, no. 29, pp. 6247–6252, 2016.

[24] L. P. Ma, W. C. Ren, Z. L. Dong, L. Q. Liu, and H. M. Cheng, "Progress of graphene growth on copper by chemical vapor deposition: Growth behavior and controlled synthesis," *Chinese Science Bulletin*, vol. 57, no. 23, pp. 2995–2999, 2012.

[25] I. Vlassiouk, M. Regmi, P. Fulvio, S. Dai, P. Datskos, G. Eres, and S. Smirnov, "Role of hydrogen in chemical vapor deposition growth of large single-crystal graphene," *ACS Nano*, vol. 5, no. 7, pp. 6069–6076, 2011.

[26] K. W. C., "The sublimation of metals at low pressures," *National Physical Laboratory*, vol. 89, no. 607, pp. 58–67, aug 1913. [Online]. Available: https://royalsocietypublishing.org/

[27] I. Vlassiouk and S. Smirnov, "Published in J. Phys. Chem. C Graphene Nucleation Density on Copper: Fundamental Role of Background Pressure," *J. Phys Chem*, vol. 18919, no. 117, pp. 1–14, 2013.

[28] P. Braeuninger-Weimer, B. Brennan, A. J. Pollard, and S. Hofmann, "Understanding and Controlling Cu-Catalyzed Graphene Nucleation: The Role of Impurities, Roughness, and Oxygen Scavenging," *Chemistry of Materials*, vol. 28, no. 24, pp. 8905–8915, 2016.

[29] C. Mattevi, H. Kim, and M. Chhowalla, "A review of chemical vapour deposition of graphene on copper," *Journal of Materials Chemistry*, vol. 21, no. 10, pp. 3324–3334, mar 2011.

[30] A. C. Ferrari and D. M. Basko, "Raman spectroscopy as a versatile tool for studying the properties of graphene," *Nature Nanotechnology*, vol. 8, no. 4, pp. 235–246, 2013. [Online]. Available: http://dx.doi.org/10.1038/nnano.2013.46

[31] C. Cong, T. Yu, and H. Wang, "Raman study on the G mode of graphene for determination of edge orientation," *ACS Nano*, vol. 4, no. 6, pp. 3175–3180, 2010.

[32] S. Reich and C. Thomsen, "Raman spectroscopy of graphite," *Philosophical Transactions of the Royal Society A: Mathematical, Physical and Engineering Sciences*, vol. 362, no. 1824, pp. 2271–2288, 2004.

[33] D. Graf, F. Molitor, K. Ensslin, C. Stampfer, A. Jungen, C. Hierold, and L. Wirtz, "Spatially resolved raman spectroscopy of single- and few-layer graphene," *Nano Letters*, vol. 7, no. 2, pp. 238–242, 2007.

[34] A. Ismach, C. Druzgalski, S. Penwell, A. Schwartzberg, M. Zheng, A. Javey, J. Bokor, and Y. Zhang, "Direct chemical vapor deposition of graphene on dielectric surfaces," *Nano Letters*, vol. 10, no. 5, pp. 1542–1548, 2010.

[35] N. Yoshihara and M. Noda, "Chemical etching of copper foils for single-layer graphene growth by chemical vapor deposition," *Chemical Physics Letters*, vol. 685, pp. 40–46, 2017. [Online]. Available: https://www.sciencedirect.com/science/article/pii/S0009261417307054

[36] N. C. Vieira, J. Borme, G. MacHado, F. Cerqueira, P. P. Freitas, V. Zucolotto, N. M. Peres, and P. Alpuim, "Graphene field-effect transistor array with integrated electrolytic gates scaled to 200 mm," *Journal of Physics Condensed Matter*, vol. 28, no. 8, p. 85302, 2016. [Online]. Available: http://dx.doi.org/10.1088/0953-8984/28/8/085302

[37] L. Gao, W. Ren, H. Xu, L. Jin, Z. Wang, T. Ma, L.-P. Ma, Z. Zhang, Q. Fu, L.-M. Peng, X. Bao, and H.-M. Cheng, "Repeated growth and bubbling transfer of graphene with millimetre-size single-crystal grains using platinum." *Nature communications*, vol. 3, p. 699, feb 2012.

[38] Y. Wang, Y. Zheng, X. Xu, E. Dubuisson, Q. Bao, J. Lu, and K. P. Loh, "Electrochemical delamination of CVD-grown graphene film: toward the recyclable use of copper catalyst." *ACS nano*, vol. 5, no. 12, pp. 9927–9933, dec 2011.

[39] F. Pizzocchero, B. S. Jessen, P. R. Whelan, N. Kostesha, S. Lee, J. D. Buron, I. Petrushina, M. B. Larsen, P. Greenwood, W. J. Cha, K. Teo, P. U. Jepsen, J. Hone,

P. Bøggild, and T. J. Booth, "Non-destructive electrochemical graphene transfer from reusable thin-film catalysts," *Carbon*, vol. 85, pp. 397–405, 2015. [Online]. Available: https://www.sciencedirect.com/science/article/pii/S0008622314012226

[40] Z. Zhu, P. Chen, K. Liu, and C. Escobedo, "A versatile bonding method for PDMS and SU-8 and its application towards a multifunctional microfluidic device," *Micromachines (Basel)*, vol. 7, no. 12, p. 230, Dec. 2016.

[41] J. Gu, X. Li, H. Ma, Y. Guan, and Y. Zhang, "One-step synthesis of PHEMA hydrogel films capable of generating highly ordered wrinkling patterns," *Polymer*, vol. 110, pp. 114–123, feb 2017.

[42] T. Webb, *Black Magic 2-inch System Manual*, rev1.1 ed., mar 2010.

[43] I. K. Liapis, "Schirmer tear and fluorescein tests," *Hellenic Journal of Companion Animal Medicine*, vol. 4, no. 2, pp. 63–70, dec 2015. [Online]. Available: https://hjcam.hcavs.gr/index.php/hjcam/article/view/83

[44] K. N. Gelatt and E. O. MacKay, "Distribution of intraocular pressure in dogs," *Veterinary Ophthalmology*, vol. 1, no. 2-3, pp. 109–114, 1998.

[45] C. Maldonado-Codina and N. Efron, "Impact of manufacturing technology and material composition on the mechanical properties of hydrogel contact lenses," *Ophthalmic and Physiological Optics*, vol. 24, no. 6, pp. 551–561, nov 2004. [Online]. Available: https://onlinelibrary.wiley.com/doi/full/10.1111/j.1475-1313.2004.00236.xhttps://onlinelibrary.wiley.com/doi/abs/10.1111/j.1475-1313.2004.00236.xhttps://onlinelibrary.wiley.com/doi/10.1111/j.1475-1313.2004.00236.x

[46] E. Oyarce, G. D. C. Pizarro, D. P. Oyarzún, C. Zúñiga, and J. Sánchez, "HYDROGELS BASED ON 2-HYDROXYETHYL METHACRYLATE: SYNTHESIS, CHARACTERIZATION AND HYDRATION CAPACITY," *J. Chil. Chem. Soc*, vol. 65, p. 1, 2020.

[47] H. Rashid, M. Ahmad, M. U. Minhas, M. Sohail, and M. F. Aamir, "Synthesis and characterization of poly(hydroxyethyl methacrylate-co-methacrylic acid) cross linked polymeric network for the delivery of analgesic agent," pp. 999–1007, 2015. [Online]. Available: https://www.researchgate.net/publication/290456548_Synthesis_and_characterization_of_polyhydroxyethyl_methacrylate-co-methacrylic_acid_cross_linked_polymeric_network_for_the_delivery_of_analgesic_agent

[48] C. Alvarez-Lorenzo, F. Yañez, R. Barreiro-Iglesias, and A. Concheiro, "Imprinted soft contact lenses as norfloxacin delivery systems," *Journal of Controlled Release*, vol. 113, no. 3, pp. 236–244, 2006.

[49] "Hyaluronic Acid 161 — MakingCosmetics." [Online]. Available: https://www.makingcosmetics.com/HUM-HYAL-01.html?lang=default

[50] Anita Nelson, "DNAshopper Hyaluronic Acid Mixing," 2009. [Online]. Available: www.modelsupplies.info

A

Recipes

Listing A.1: Optimized recipe used for graphene growth and initial testings.

```
1   COMM H2, CH4 and Ar
2   TUNE PCON Fully open
3   VALV 1 OPEN
4   FLOW 3 ON 0
5   WAIT PRES < 0.20
6   FLOW 2 ON 1500
7   WAIT TIME > 120
8   FLOW 2 OFF
9   WAIT PRES < 0.15
10  FLOW 2 ON 1500
11  WAIT TIME > 120
12  FLOW 2 OFF
13  WAIT PRES < 0.10
14  FLOW 1 ON 20
15  FLOW 2 ON 560
16  VALV 1 CLOSE
17  TUNE PCON graphene at 20mbar
18  PCON ON 20 1
19  TUNE HTTC zero power
20  HEAT ON 800.0 200.0
21  TUNE HTTC standard monolayer graphene 500C - 2''
22  WAIT TEMP > 475.0
23  TUNE HTTC standard monolayer graphene 675C - 2''
24  WAIT TEMP > 650.0
25  TUNE HTTC 800C - 2" stable
26  WAIT TEMP > 740.0
27  TUNE HTTC 900C - 2" heater test
28  WAIT TEMP > 790.0
29  TUNE HTTC 900C - thin 1"
30  HEAT ON 825.0 7.0
```

```
31  WAIT TEMP > 815.0
32  WAIT TIME > 600
33  FLOW 3 ON 10
34  WAIT TIME > 600
35  FLOW 3 OFF
36  HEAT ON 275.0 200.0
37  WAIT TEMP < 655.0
38  TUNE HTTC standard monolayer graphene 675C - 2''
39  WAIT TEMP < 505.0
40  TUNE HTTC standard monolayer graphene 500C - 2''
41  WAIT TEMP < 300.0
42  HEAT OFF
43  WAIT TEMP < 150.0
44  VALV 1 OPEN
45  FLOW 1 OFF
46  FLOW 2 OFF
47  WAIT PRES < 0.20
48  PCON OFF
```

Listing A.2: Recipe used for temperature testing.

```
1   COMM H2, CH4 and Ar
2   TUNE PCON Fully open
3   FLOW 3 ON 0
4   WAIT PRES < 0.20
5   TUNE PCON graphene at 20mbar
6   PCON ON 20 1
7   TUNE HTTC zero power
8   HEAT ON 800.0 200.0
9   TUNE HTTC standard monolayer graphene 500C - 2''
10  WAIT TEMP > 475.0
11  TUNE HTTC standard monolayer graphene 675C - 2''
12  WAIT TEMP > 650.0
13  TUNE HTTC 800C - 2" stable
14  WAIT TEMP > 700.0
15  HEAT ON 900.0 50.0
16  TUNE HTTC 900C - 2" heater test
17  WAIT TEMP > 810.0
18  TUNE HTTC 900C - thin 1"
19  HEAT ON 950.0 7.0
20  WAIT TEMP > 850.0
21  WAIT TIME > 60
22  HEAT ON 275.0 200.0
23  TUNE HTTC standard monolayer graphene 675C - 2''
24  WAIT TEMP < 655.0
25  TUNE HTTC standard monolayer graphene 500C - 2''
26  WAIT TEMP < 505.0
27  TUNE HTTC standard monolayer graphene 300C - 2''
28  WAIT TEMP < 300.0
29  HEAT OFF
30  WAIT TEMP < 150.0
31  VALV 1 OPEN
32  WAIT PRES < 0.20
33  PCON OFF
```

Listing A.3: Main recipe used for graphene growth.

```
1   COMM H2, CH4 and Ar
2   TUNE PCON Fully open
3   VALV 1 OPEN
4   FLOW 3 ON 0
5   WAIT PRES < 0.20
6   FLOW 2 ON 1500
7   WAIT TIME > 120
8   FLOW 2 OFF
9   WAIT PRES < 0.15
10  FLOW 2 ON 1500
11  WAIT TIME > 120
12  FLOW 2 OFF
13  WAIT PRES < 0.10
14  FLOW 1 ON 20
15  FLOW 2 ON 560
16  VALV 1 CLOSE
17  TUNE PCON graphene at 20mbar
18  PCON ON 20 1
19  TUNE HTTC zero power
20  HEAT ON 800.0 200.0
21  TUNE HTTC standard monolayer graphene 500C - 2''
22  WAIT TEMP > 475.0
```

```
23  TUNE HTTC standard monolayer graphene 675C - 2''
24  WAIT TEMP > 650.0
25  TUNE HTTC 800C - 2" stable
26  WAIT TEMP > 740.0
27  TUNE HTTC 900C - 2" heater test
28  WAIT TEMP > 790.0
29  TUNE HTTC 900C - thin 1"
30  HEAT ON 825.0 7.0
31  WAIT TEMP > 815.0
32  WAIT TIME > 600
33  FLOW 3 ON 10
34  WAIT TIME > 600
35  FLOW 3 OFF
36  HEAT ON 275.0 200.0
37  TUNE HTTC standard monolayer graphene 675C - 2''
38  WAIT TEMP < 655.0
39  TUNE HTTC standard monolayer graphene 500C - 2''
40  WAIT TEMP < 505.0
41  TUNE HTTC standard monolayer graphene 300C - 2''
42  WAIT TEMP < 300.0
43  HEAT OFF
44  WAIT TEMP < 150.0
45  VALV 1 OPEN
46  FLOW 1 OFF
47  FLOW 2 OFF
48  WAIT PRES < 0.20
49  PCON OFF
```

B

Milling Drilling Protocol

MILLING/DRILLING PROTOCOL

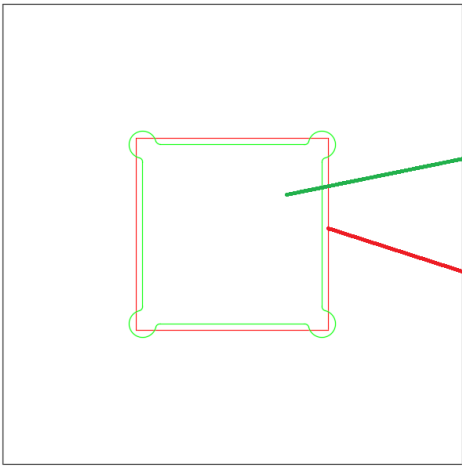**User**: Carlos Carreira / Mariana Otero / Catarina Jones   **Date**:17/08/2022

Filename: 5mmPMMA_2p8mm_pocket

Autocad Drawing [mm]   Files of type: AutoCAD 2000/LT2000 DXF (*.dxf)   ▼

100 x 100 x 5 mm^2

Pocket
Endmill 3 mm D 2.8 mm

Contour, none
Endmill 3mm D 0.5mm

Total size Width_X × Length_Y [mm]: 100 × 100	Thickness of PMMA Plate [mm]: 5

Toolpath strategy Pocket | Drill | Contour (*right | cut out | left*)	Tool Endmill | Drill	Diameter [*mm*]	Depth [*mm*]	Estimated time [*min*]
1p1_Pocket	Endmill	3	2.8	
1p2_Contour, none	Endmill	3	0.5	

INESC MN
Microsistemas e
Nanotecnologias

C

Code for image processing

Listing C.1: MATLAB Code for image processing that outputs RPM from the videos

```matlab
1 clear all
2 clc
3 cd("Videos");
4 dirVideos = dir('*.avi');
5 fileNames = {dirVideos.name}; %create cell array of file names
6 rFolder = cd; %store current directory
7
8 for iVid = 1:numel(fileNames) %loop over all videos
9
10 file_name = char(fileNames(iVid)); %current video
11 video = VideoReader(file_name);
12 v2 = VideoReader(file_name);
13 A(:,1) = 1:v2.NumberOfFrames;
```

```matlab
14  A(:,2) = zeros(v2.NumberOfFrames,1);

15

16  newFolder = sprintf('%s', v2.Name(1:end-6));  % name of new folder
17  mkdir(newFolder);                             % creates folder to store files
18  cd(newFolder);                                % changes directory to new folder
19  % move video to new folder
20  movefile(fullfile(rFolder,file_name),fullfile(pwd,file_name));

21

22  figure(1)
23  imshow(rgb2gray(readFrame(video)));
24  [X,Y] = ginput(1);
25  print(figure(1),'Gray_FirstFrame','-dpng')

26

27  i=1;

28

29  while hasFrame(video)
30      frame = readFrame(video);
31      image_grey = rgb2gray(frame);
32      A(i,2) = image_grey(round(Y),round(X));
33      i = i+1;
34  end

35

36  figure(2)
37    subplot(1,2,1)
38    plot(A(:,1), A(:,2),'-*')
39    title(v2.Name)
40    xlabel('frame nr'); ylabel('Greyscale intensity')

41

42    subplot(1,2,2)
43    FrameRate = 30; %frames per second
44    plot(A(:,1)/FrameRate, A(:,2),'-*')
45    title(v2.Name)
46    xlabel('time [s]'); ylabel('Greyscale intensity')
47    print(figure(2),'GrayscaleI_time_frameNr','-dpng')

48

49  x = A(:,2);                   % Variable
50  SampleRateHZ = FrameRate;     % Sampling frequency
51  Ts = 1/SampleRateHZ;          % Sample time
```

```matlab
52  L = size(x,1);                    % Length of signal
53  t = (0:L-1)*Ts;                   % Time vector
54
55  % Modification of values to a set value under and above a treshold
56
57  for i = 1:L
58      if x(i) < 215
59          x(i) = 10;
60      else
61          x(i) = 250;
62      end
63  end
64
65  figure(3)
66     plot(A(1:length(x),1)/FrameRate, x,'-*')
67     title(v2.Name)
68     xlabel('time [s]'); ylabel('Grayscale intensity')
69  print(figure(3),'GrayscaleI_time_Xnorm','-dpng')
70
71  NFFT = 2^nextpow2(L); % Next power of 2 from length of y
72  F = fft(x,NFFT)/L; % FFT
73
74  % Plot single-sided amplitude spectrum.
75  figure(4)
76      subplot(1,2,1)
77      Frequency=2*abs(F(1:NFFT/2+1));
78      %w= SampleRateHZ./NFFT.*(0:size(Frequency,1));
79      w = SampleRateHZ/2*linspace(0,1,NFFT/2+1);
80
81      plot(w(10:end),Frequency(10:end))
82      title('Single-Sided Amplitude Spectrum of x(t)')
83      xlabel('Frequency (Hz)'); ylabel('Magnitude of Fourier Coefficients |F(w)|')
84
85      hold on;
86      NCell=textscan(file_name,'%s','Delimiter','_');
87      NFR=char(NCell{1,1}(2));
88      FeedR=str2num(NFR(2:end));
89      FN=FeedR/110;
```

```matlab
90      nn=max(10,find(w>=FN,1));
91      index=find(Frequency==max(Frequency((nn:NFFT/2+1))));
92      mainFrequencyStr=num2str(w(index(1)));
93      mainCoefficientStr=num2str(Frequency(index(1)));
94      plot(w(index(1)),Frequency(index(1)),'r.', 'MarkerSize',25);
95      text(w(index(1))+2,Frequency(index(1)),[' (' ,mainFrequencyStr,', ',
           mainCoefficientStr,')']);
96      title(['The rotational conditions for ' v2.Name ' resulted in ',num2str(w(
           index(1))*60),' rpm']);
97      hold off;
98
99
100 % Plot power spectrum
101     subplot(1,2,2)
102     power = F.*conj(F)./NFFT;
103     plot(w(10:end), power(10:end/2+1));
104     xlabel('Frequency (Hz)')
105     ylabel('Power')
106
107     hold on;
108     index2=find(power==max(power(nn:NFFT/2+1)));
109     mainfreqStr=num2str(w(index2(1)));
110     mainPowerStr2=num2str(power(index2(1)));
111     plot(w(index2(1)),power(index2(1)),'r.', 'MarkerSize',25);
112     text(w(index2(1))+2,power(index2(1)),['(',mainfreqStr,', ',mainPowerStr2,')'
           ]); % +2 to write @ 2 points distance from YY axis
113     hold off;
114     print(figure(4),'SSamplitudeSpectr_PowerSpectr','-dpng')
115     cd(rFolder) % changes back to videos folder
116
117     num2str(w(index(1))*60)
118     clear A
119
120 end
```

D

Runsheet for graphene transfer

GRAPHENE EXTRACTION

| **Step 1:** PMMA spin coating	**Time:**	**Date:**	**Responsible:**
Location: Clean room/Yellow room			

1) **Substrate**: graphene-Cu film, Si wafer
2) **Equipment:** SVG Track, Hot plate, PMMA beaker
3) **Procedure:**

    3.1 Tape the graphene-Cu film into a plastic surface

    3.2 Clean Si wafer (from wafer box labelled "PMMA only") with acetone and blow dry

    3.3 Tape the plastic surface with Cu substrate onto the Si wafer

    3.4 Place the wafer in place on the SVG

    3.5 Manually add PMMA 950 (aim for the center of the graphene-Cu substrate)

    3.6 Spin coat PMMA: 600 nm (Recipe 3) @ SVG

Step description	Coating Parameters
First step	spin @ 0 rpm for 10 s to descend the wafer and add the PMMA manually
Second step	spin @ 3 krpm, 10 krpms^{-1},for 30 s to spread the PMMA
Third step	EBR @ 1.5 krpm for 5s spin @ 1.5 krpm for 10s

    3.7 Bake at **160°C** for 4 min to improve PMMA adhesion

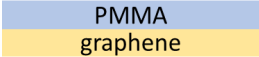   3.8 After substrate cool down, **REPEAT** step 6 to get a double layer of PMMA

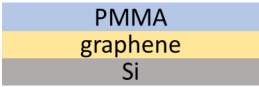- Use a droplet of DI water and clean room paper to flatten the Cu foil [STEP 1]

4) Sample scheme:

| PMMA |
|---|
| graphene |
| Cu |
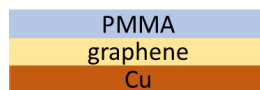
Observations/Comments:

Step 2: Cu chemical etching **Location:** Clean room	**Time:**	**Date:**	**Responsible:**

1) **Substrate**: PMMA/graphene/Cu films
2) **Equipment:** Hot plate, tweezers, beaker
3) **Procedure:**
   - 3.1 Prepare a solution of 0.5M $FeCl_3.6H_2O$
   - 3.2 Heat the solution to 35/40°C
   - 3.3 Place the sample in the solution of $FeCl_3$ (make sure the PMMA side is facing up) and leave it on the hot plate for 1h.

4) Sample scheme:

PMMA
graphene

Observations/Comments:

Step 3: Sample cleaning and fishing	**Time:**	**Date:**	**Responsible:**
Location: Clean room/Grey area			

1) **Substrate**: PMMA/graphene film; glass slide; Dehydrated hydrogel
2) **Equipment**: Tweezers, beakers, glass slide
3) **Procedure**:
   - 3.1 Clean the **glass slide** with acetone, IPA, rinse with DI water and blow dry
   - 3.2 Fish the PMMA/graphene film with the glass slide **from the FeCl₃ solution into** a beaker with **DI water** and leave it for **10 min**
   - 3.3 Transfer the PMMA/graphene sample into a **HCl (2%) solution** and leave it **for 30 min**
   - 3.4 **Perform the transfer** of the sample between HCl (2%) and DI water **3 times**
   - 3.5 Fish the sample from the DI water with **final** substrate
   - 3.6 Leave the sample to dry at room temperature overnight to improve adhesion

   - Always rinse the glass slide with DI water before fishing the substrate [STEP 4]
4) Sample scheme:

PMMA
graphene
Si

Observations/Comments:

Step 4: PMMA removal	**Location:** Clean room	**Time:**	**Date:**	**Responsible:**

1) **Substrate**: PMMA/graphene film on Hydrogel; glass slide
2) **Equipment**: beakers
3) **Procedure:**
    3.1 Immerse the sample in an acetone bath for 1h
    3.2 Rinse with IPA, DI water and blow dry with compressed air
4) Final substrate scheme:

<div align="center">

graphene
Si

</div>

Observations/Comments:

E
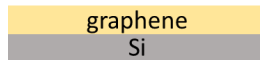
In-vivo related documents

Exma. Senhora
Professora Doutora Esmeralda Delgado
Faculdade de Medicina Veterinária

Lisboa, 29 de setembro de 2022

Assunto: Avaliação projeto de investigação – N/Refª 016/2022

Vimos pela presente informar V.Exa. que a CEIE, após ter avaliado as atividades que envolvem manipulação de animais, no âmbito do projeto de investigação "Biocompatibilidade e tolerância de um inserto ocular microfluídico a nível tópico ocular em cães – projeto piloto" considerou que estão salvaguardados os princípios éticos e de bem-estar animal exigidos pela legislação vigente e pelo código de boas práticas, pelo que aprovou a execução do protocolo experimental nas instalações e serviços da FMV, conforme requerido por V.Exa.

Com os melhores cumprimentos,

Graça Ferreira Dias
Coordenadora da Comissão de Ética para a Investigação e Ensino

Consentimento informado para participação em estudo científico

Eu, _Raquel Bastos_ ,

portador(a) do CC nº _13336275_ , tutor(a) do canídeo de nome _Sansa_ ,

de raça _podengo_ , sexo _♀_ e idade _8_ , declaro que fui informado e que

autorizo a participação no projeto "**Biocompatibilidade e tolerância de um inserto ocular microfluidico a nível tópico ocular em cães – projeto piloto.**", autorizando:

X A colocação do inserto ocular

X Realização de acompanhamento oftalmológico durante o ensaio

X Colheita de dados clínicos e outras informações

X obternção de fotografias

Fui também informado dos procedimentos e condições necessários à realização do estudo:

• Concordei com a colocação do inserto ocular no meu animal

• Irei a consultas de reavaliação durante o tempo de realização do ensaio

.• A privacidade dos dados dos proprietários incluídos no ensaio será respeitada no caso dos resultados serem utilizados em comunicações escritas ou orais.

• Estou ciente que posso desistir do estudo a qualquer momento.

Deste modo dou fé de:

• Ter lido a informação que me foi entregue.

• Ter podido fazer as perguntas que entendi por necessárias sobre o estudo.

• Ter recebido informação suficiente sobre o estudo.

Lisboa, _17_ de _outubro_ , de 2022 _____

(Assinatura do/a tutor/a) _Raquel Bastos_ _____

As informações pessoais recolhidas destinam-se exclusivamente ao projeto e poderão ser utilizadas em âmbito educativo. As informações estão sujeitas a processamento informático para monitorização do estudo e serão guardadas por um período de 20 anos. De acordo com os regulamentos relativos a dados pessoais, tem o direito de aceder, retificar e limitar o processamento e portabilidade dos seus dados. Antes do início do estudo poderá anular o consentimento e solicitar a eliminação dos seus dados.